

Received 16 March 2025, accepted 14 April 2025, date of publication 21 April 2025, date of current version 22 May 2025.

Digital Object Identifier 10.1109/ACCESS.2025.3563115

SURVEY

PWM Techniques for Two-Level Voltage Source Inverters: A Comparative Study

BATTUR BATHKISHIG¹, (Member, IEEE), **PEDRO F. DA COSTA GONÇALVES²**, (Member, IEEE), **GIORGIO PIETRINI¹**, (Member, IEEE), **BABAK NAHID-MOBARAKEH¹**, (Fellow, IEEE), AND **ALI EMADI¹**, (Fellow, IEEE)

¹McMaster Automotive Resource Centre (MARC), McMaster University, Hamilton, ON L8P 0A6, Canada

²Vestas Wind Systems A/S, 8200 Aarhus, Denmark

Corresponding author: Battur Bathkishig (bathkish@mcmaster.ca)

This work was supported in part by MITACS.

ABSTRACT Pulse width modulation (PWM) techniques are widely used to control the switching of semiconductors in power converters. This paper presents a comprehensive overview of PWM techniques for two-level voltage source inverters and provides a comparative analysis of commonly employed PWM techniques, including sinusoidal PWM, zero-sequence injection PWM, third-harmonic injection PWM, space vector modulation, and optimized pulse pattern with selective harmonic mitigation. Besides providing a detailed literature review, this study includes multiple experimental results to evaluate the performance of these PWM techniques across different key metrics, such as output power quality, DC-link voltage utilization, dynamic response, and complexity. Given the growing trend of electrification in the transportation sector, particular emphasis is placed on motor drive applications. Furthermore, this paper discusses the impact of digital controllers, wide-bandgap semiconductors, and model predictive control on PWM techniques while addressing the challenges and future trends within this field.

INDEX TERMS Carrier-based pulse width modulation (PWM), pre-programmed PWM, space vector modulation, total harmonic distortion, voltage source inverter.

NOMENCLATURE

C_{dc}	DC-link capacitor.
I_1	Fundamental component of phase current.
I_n	Amplitude of n^{th} order current harmonic component.
$P_{sw,norm}$	Normalized switching loss.
$THD_{I,6s}$	Phase current total harmonic distortion at six-step operation.
THD_I	Phase current total harmonic distortion.
T_d	Deadtime.
V_1	Fundamental output voltage.
V_{dc}	DC-link voltage source.
V_n	Amplitude of n^{th} order voltage harmonic component.
V_{ref}	Reference voltage vector.
V_x^*	Resultant modulating signals.

$WTHD_V$	Weighted voltage total harmonic distortion.
f_1	Fundamental frequency.
f_{sw}	Switching frequency.
m_f	Switching-to-fundamental frequency ratio.
m_i	Output modulation index, $0-4/\pi$.
m_i^*	Reference modulation index.
v_x^*	Reference modulating signals.
α_x	Optimal switching angles.
θ_u	Reference voltage angle.
L	Inductive load.
M	Maximum harmonic order.
N	Number of switching actions.
R	Resistive load.
MI	Normalized output modulation index, 0-1.
d	Distortion factor.

I. INTRODUCTION

The associate editor coordinating the review of this manuscript and approving it for publication was Jorge Esteban Rodas Benítez¹.

In recent years, advances in semiconductor technologies have propelled the widespread adoption of power converters across

diverse applications [1], [2]. The large variety of applications has created diverse requirements, prompting the development of numerous DC/AC power converter topologies. These include two-level voltage source inverters (2L-VSIs), current source inverters (CSIs), as well as multilevel inverters such as cascaded H-bridge (CHB), neutral point clamped (NPC), and flying capacitor (FC) [3].

Among these converters, three-phase 2L-VSIs have emerged as one of the most commonly used power converter topologies, widely employed across a broad spectrum of applications, such as grid [4], [5], renewable energy [6], motor drive [7], [8], industry [9], uninterruptible power supply (UPS) [10], [11], and photovoltaic systems [12], [13], [14], [15]. The widespread adoption of 2L-VSIs is attributed to their straightforward topology, high efficiency, low cost, good dynamic response, high power density, and well-established pulse width modulation (PWM) techniques [16]. However, the varying requirements and performance criteria across different applications demand optimized performance of VSI for specific use cases. Consequently, optimizing the performance of VSIs to match particular applications has become an essential topic of study.

The performance of VSIs is highly contingent on the pulse width modulation (PWM) technique utilized. Therefore, selecting the appropriate PWM technique plays a significant role in attaining the desired performance in the VSI. Over the last decades, many PWM techniques have been developed in various research works, focusing on improvements in specific performance criteria [17], [18], [19], [20], [21], [22], [23]. As a result, identifying the most suitable PWM technique for a given application becomes crucial to meet particular performance requirements.

Although distinct applications may entail different performance demands, better output power quality for a given switching frequency, broader operational range, simplicity, and capability to change the output voltage quickly are general performance criteria for PWM techniques in almost all applications. The significance of each criterion varies depending on the specific application, and additional performance criteria may also be considered. Beyond defining the desired performance indices, understanding the concepts and features of PWM techniques is imperative to determine which PWM technique can deliver optimal performance.

Over the years, numerous review articles have been published on PWM techniques, offering detailed discussions of their principles, classifications, and application-specific features. For instance, [24] surveys classical PWM methods and current tracking control strategies for AC motor drives, with particular emphasis on the impact of switching time delays. In [25], various gate signal generation methods are explored for both multi-level and 2L-VSIs, encompassing classical PWM, pseudo-modulation schemes, and closed-loop control techniques with modulators. Meanwhile, [26] and [27] focus on specialized topics, such as PWM strategies for common mode voltage mitigation and pre-programmed

PWM techniques tailored for high-power AC motor drives, respectively. Most existing reviews tend to focus on theoretical concepts, recent state-of-the-art advancements, specific PWM categories, or particular performance metrics, often lacking comprehensive experimental validation across a broader operational range. This paper addresses that gap by presenting a comparative overview and a side-by-side performance evaluation of commonly used PWM techniques for 2L-VSIs, including sinusoidal PWM (SPWM), zero sequence injection PWM (ZSI-PWM), third harmonic injection PWM (THI-PWM), space vector modulation (SVM), and selective harmonic mitigation (SHM), supported by experimental results. By adopting broader experimental conditions, a fair comparison has been ensured while showcasing the effective operating conditions of each PWM technique. In addition to offering a side-by-side comparison of key performance indices, this paper provides practical insights into the challenges and advantages of each PWM technique based on hardware implementations and complexity, highlighting their limitations and hardware requirements. Finally, the existing challenges, new requirements, model predictive control (MPC), the influence of hardware advancements, and multiphase VSIs are discussed to predict potential future trends in PWM techniques, followed by the conclusion of this study.

The main contributions of this paper are summarized as follows:

- Preferent PWM generation concepts, along with a review of the most commonly used techniques for each concept.
- Discusses key performance indices of PWM techniques, including harmonic performance, DC-link utilization, dynamic response, and complexity.
- Offers a side-by-side experimental comparison of commonly used PWM techniques across a broader range of operating conditions, providing an unbiased evaluation based on key performance indices.
- Highlights the drawbacks and advantages of each PWM technique, considering their hardware requirements and complexity.
- Discusses emerging trends in PWM techniques, focusing on their existing challenges, new requirements, advanced controls, and hardware advancements.

II. THREE-PHASE TWO-LEVEL VOLTAGE SOURCE INVERTER

The topology of a three-phase 2L-VSI is illustrated in Fig. 1. This topology is comprised of three individual half-bridges, each equipped with freewheeling diodes, all connected in parallel to a common DC voltage source V_{dc} and capacitor C_{dc} . 2L-VSI is considered as a standard DC/AC converter and is widely used in many applications due to its simple structure, low cost, high-efficiency, and high-power density. These features made 2L-VSIs the primary choice in motor drive systems, notably in the electrified transportation sector, where the cost, power density, and efficiency are paramount [28].

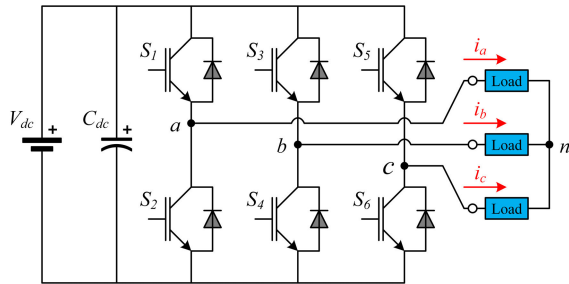


FIGURE 1. The circuit diagram of a 2L-VSI connected with loads.

The main functionality of 2L-VSIs is to convert the input DC-link voltage into a three-phase output AC voltage with variable magnitude, phase shift, and frequency. This conversion relies on the precise control of the ON and OFF time duration of each switching device. This timing of the switches is controlled by trains of pulses with different widths using PWM techniques. Subsequently, PWM techniques have been studied extensively to allow precise control over the inverter.

III. PERFORMANCE INDICES

The selection of PWM techniques profoundly influences various performance aspects of the VSIs, including output power quality, efficiency, switching losses, reliability, operating range, and lifetime. Hence, meticulous selection of the appropriate PWM technique for a specific application and topology is crucial in maximizing performance and efficiency on both the inverter and the load. To facilitate this selection process, it becomes imperative to determine the key performance indices tailored to the application at hand. This section discusses the critical key performance indices associated with PWM techniques for 2L-VSIs.

A. HARMONIC PERFORMANCE

PWM-controlled VSIs inherently produce discrete output voltage waveforms, introducing undesired harmonic distortions into the output voltages and currents. These harmonic distortions can significantly deteriorate the output power quality and negatively affect the load connected to the inverter. While this issue can be mitigated by increasing the switching frequency of VSIs, it also leads to increased switching losses, reducing VSI efficiency. Thus, achieving lower harmonic distortions for a given switching frequency is paramount. Consequently, harmonic performance emerges as an utmost important criterion in evaluating PWM techniques. Therefore, quantifying the quality of output power produced by VSIs is necessary [29]. In many applications, including motor drives, current distortion holds particular significance over voltage harmonics due to its direct impact on machine losses and torque ripple [30], [31]. The total harmonic distortion (THD) stands as an essential key metric for assessing the quality of inverter output phase currents and

voltage, computed as:

$$THD_I = \frac{\sqrt{\sum_{n=2}^M (I_n)^2}}{I_1} \times 100\%, \quad (1)$$

where I_1 denotes the amplitude of the fundamental current component of a phase, I_n represents the amplitude of the n^{th} -order current harmonic component of a phase, and M is the maximum harmonic order. However, it is noteworthy that current THD is contingent upon the load impedance. To mitigate load dependency, the current THD is normalized against the current THD of the six-step mode operation $THD_{I,6s}$, yielding the current distortion factor [32], [33]:

$$d = THD_I / THD_{I,6s}. \quad (2)$$

Furthermore, the weighted total harmonic distortion (WTHD) is an effective metric for evaluating the quality of output current solely based on voltage waveforms [34]. By introducing a weight factor of $1/n$, WTHD offers an approximation of current THD specifically tailored for inductive loads. This weight factor attenuates the significance of higher-order harmonics, which are dampened by the low-pass filtering characteristics of inductive loads [34]. Given its ability to derive current THD directly from voltage waveforms, WTHD finds widespread application in analyzing the harmonic performance of VSIs utilized in motor drive applications since motors are predominantly inductive loads [35], [36]. Therefore, WTHD emerges as a valuable tool in assessing the harmonic performance of PWM techniques as it uses voltage waveforms directly. WTHD is calculated as:

$$WTHD_V = \frac{\sqrt{\sum_{n=2}^M \left(\frac{V_n}{n}\right)^2}}{V_1} \times 100\%, \quad (3)$$

where V_1 denotes the amplitude of a phase fundamental voltage component while V_n is denoting the amplitude of the n^{th} -order voltage harmonic component of a phase.

B. DC-LINK VOLTAGE UTILIZATION

The theoretical maximum output voltage V_1 of 2L-VSIs, which maintains an equivalent mean average to the fundamental component, based on the six-step mode, for a given input DC-link voltage V_{dc} , without considering deadtime effects, is defined as [37]:

$$V_1 = \frac{2}{\pi} \times V_{dc}. \quad (4)$$

As the magnitude of the DC-link voltage varies among different VSIs, using the actual output voltage value is not suitable for quantifying the DC-link voltage utilization rate. To address this issue, the output voltage for the given DC-link voltage is often normalized by (4) as follows [38]:

$$MI = \frac{V_1}{2/\pi \times V_{dc}}, \quad 0 < MI < 1. \quad (5)$$

However, in most research works, PWM technique performance and VSI operating points are typically represented as a function of the modulation index m_i , calculated by dividing the amplitude of the output voltage fundamental component by half of the input DC-link voltage. In this paper, the term output modulation index denotes the amplitude of the output voltage relative to the input DC-link voltage rather than the normalized output voltage MI . The output modulation index is defined as [39]:

$$m_i = \frac{V_1}{V_{dc}/2}, \left\{ 0 < m_i < \frac{4}{\pi} \right\}. \quad (6)$$

DC-link voltage utilization of PWM techniques is determined by the maximum achievable output fundamental voltage for a given DC-link voltage without a significant increase in the THD and low-order harmonic components while maintaining linearity between the output voltage amplitudes and modulating signal. Nevertheless, the linear control range for adjusting the output voltage amplitude in relation to the modulating signal amplitude varies among PWM techniques. A narrower linear operating range implies less effective utilization of the DC-link voltage. Hence, a broader linear operating region is preferable to maximize the operating points of the inverter for a given DC-link voltage. Consequently, numerous PWM techniques with extended linear operating ranges, such as the well-known SVM [17], ZSI-PWM [40], THI-PWM [19], and discontinuous PWM techniques [41], have been developed. Moreover, overmodulation strategies have been introduced to further extend the operational range of the inverter up to the six-step mode [38], [42], [43], [44]. In summary, higher DC-link voltage utilization stands as one of the most critical factors during the selection of PWM techniques.

C. DYNAMIC PERFORMANCE

The dynamic response of PWM techniques owes direct relation to the switching frequency and the execution frequency of the digital controller [45]. In closed-loop systems, however, the dynamic performance of PWM techniques is primarily dictated by the bandwidth of the closed-loop control responsible for generating modulating signals. It is noteworthy to mention that the bandwidth of the closed-loop systems is typically significantly lower than the switching frequency of the VSI [46]. Consequently, PWM techniques provide the desired voltage magnitude and frequency faster than the closed-loop response. However, the bandwidth of incorporating closed-loop controls is often reduced depending on the type of PWM employed to prevent any degradation in the harmonic performance of the PWM technique [47]. Therefore, the dynamic performance of PWM techniques primarily revolves around their suitability in closed-loop systems with high dynamic requirements.

D. COMPLEXITY

Compared to the PWM techniques designed for multi-level inverters and current source inverters, those tailored

for 2L-VSIs exhibit simplicity and are well-established methodologies [48]. Nevertheless, complexity and hardware-associated requirements remain essential factors during the PWM selection process. This article evaluates the complexity of presented PWM techniques in terms of sampling, implementation process, and hardware requirements. Generally, PWM techniques with lower computational costs are often preferred over their more complex counterparts, highlighting the importance of simplicity in PWM selection.

IV. PWM TECHNIQUES

PWM techniques operate on the main concept of modulating a reference signal, referred to as a modulating signal, by controlling the duration of turn-on and turn-off intervals of switching devices using pulses of varying widths but with the same amplitudes. This manipulation enables independent control over output voltage magnitude, phase shift, and fundamental frequency. However, PWM techniques can be classified depending on the fundamental principle of generating pulses, as illustrated in Fig. 2.

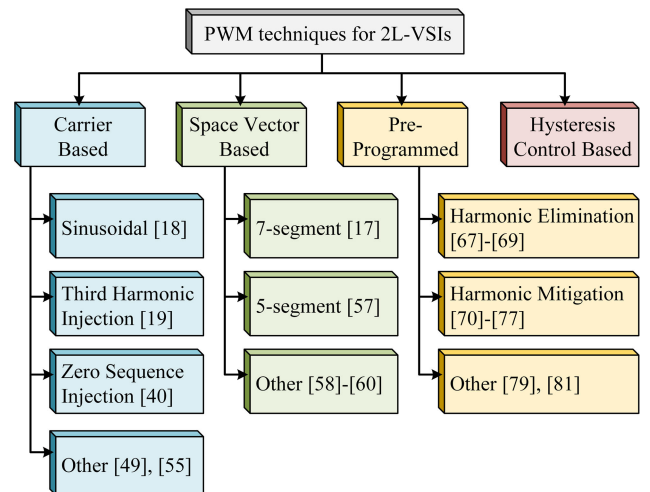


FIGURE 2. Classification of PWM techniques based on their pulse generation principles.

A. CARRIER-BASED PULSE WIDTH MODULATION

Carrier-based PWM (CBPWM) techniques generate pulses by comparing reference waveforms with a high-frequency carrier waveform. The reference and carrier signals can technically assume diverse shapes and forms to achieve desired performance outcomes [49], [50]. However, among many CBPWM techniques, SPWM stands out as one of the most fundamental and widely recognized methods due to its straightforward analog and digital implementation [51], [52]. In SPWM, the switching states are determined by comparing the three-phase 120-degree phase-shifted sinusoidal reference signals v_x^* , where $x \in \{a, b, c\}$, with a high-frequency sawtooth or triangle waveforms, as depicted in Fig. 3.

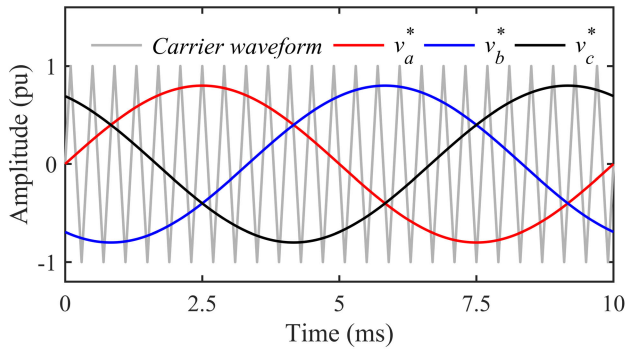


FIGURE 3. Three-phase modulating signals of sinusoidal PWM and high-frequency carrier waveform.

It is noteworthy to mention that triangle and sawtooth waveforms are predominantly used as carriers due to their simplicity and ease of implementation in practical applications. Nevertheless, compared to the sawtooth carrier waveform, the triangle carrier waveform offers less harmonic components and twice the sampling points, i.e., the measurements are sampled at the minimum and maximum points of the triangle waveform [34]. Conversely, when using the sawtooth carrier, the measurements are only sampled once per carrier period as its minimum and maximum points occur at the same time. For these reasons, the triangle carrier is frequently employed in CBPWM techniques despite its lower resolution.

Despite its popularity, SPWM can only utilize up to 78.54% of the achievable output voltage without going into the overmodulation region. The amplitude ratio of the modulating signals and carrier waveform governs the effective DC-link utilization of CBPWM techniques. This ratio, often referred to as the reference modulation index m_i^* . When the ratio of the modulating signal to the carrier waveform, or reference modulation index, exceeds 1, the number of pulses over the fundamental period decreases, resulting in nonlinear output voltage and increased lower-order harmonics due to reduced switching frequency [53]. This scenario can cause increased torque ripples, acoustic noise, and vibration, eventually leading to a fault [54]. Therefore, CBPWM techniques are conventionally utilized within their linear range where the reference modulation index is below 1.

To overcome the low DC-link utilization of SPWM, THI-PWM, ZSI-PWM, and other carrier-based PWM techniques are derived from SPWM [55]. THI-PWM and ZSI-PWM inject third-order harmonic and zero-sequence voltage into the original sinusoidal reference waveform, respectively. Following the injection of those additional signals into the sinusoidal modulating signals v_x^* , the amplitude of the resultant waveforms V_x^* decreases by 13.4% while maintaining the same fundamental output. This enables effective DC-link voltage utilization of up to 90.69%. The block diagram and resultant waveforms are illustrated in

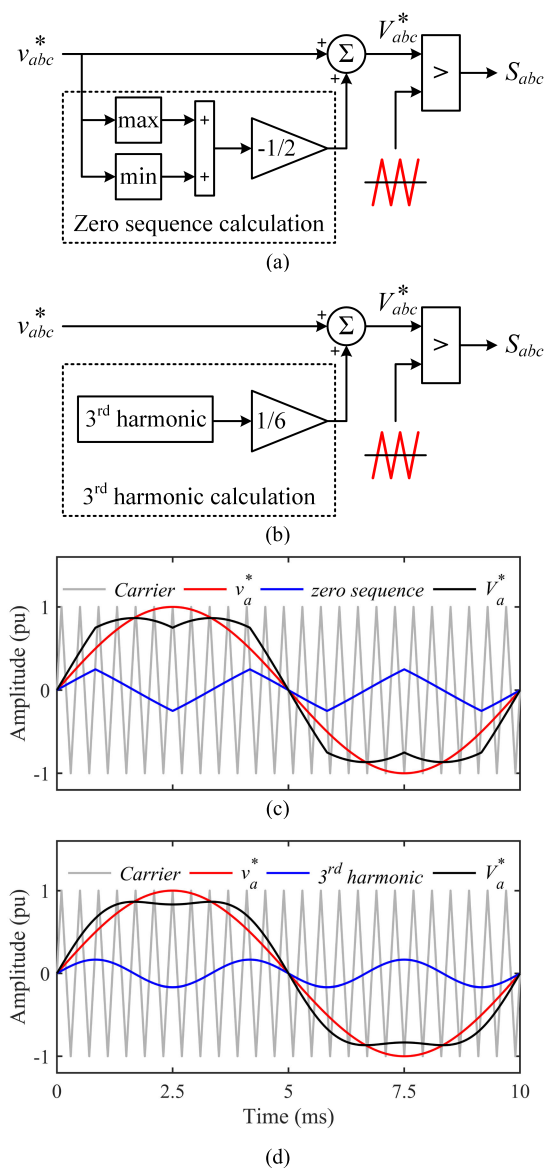


FIGURE 4. Block diagram of (a) ZSI-PWM and (b) THI-PWM, and the resultant modulating waveforms for (c) ZSI-PWM and (d) THI-PWM.

Fig. 4. These methods emerged as popular alternatives to SPWM in motor drive applications due to their enhanced DC-link voltage utilization. Notably, the ZSI-PWM technique, widely referred to as space vector PWM (SVPWM) due to its resultant waveform equivalence with SVM, is often preferred due to its simplicity in implementation.

B. SPACE VECTOR MODULATION

SVM has emerged as a popular alternative to CBPWM techniques in 2L-VSIs, finding extensive application in motor drives due to its higher DC-link utilization and enhanced harmonic performance [56]. Developed in the 1980s, SVM generates switching signals based on the space vector representation of the voltage vectors in an orthogonal stationary $\alpha\beta$ frame. In this technique, the six

active voltage vectors and two null voltage vectors, generated by the eight possible switching states of the 2L-VSI, form a hexagon divided into six sectors, as shown in Fig. 5 [17]. The primary objective of SVM is to produce the same output voltage vector as the rotating reference voltage vector V_{ref} by controlling the time duration and sequence of the switching states per sampling period. For instance, when the reference voltage vector is in sector I, the switching states change between 100, 110, 000, and 111 to approximate the reference voltage. Furthermore, by altering the switching sequence generation and dwell time calculation, SVM can achieve different performance criteria such as, reduced switching loss, improved harmonics, or common mode voltage reduction, rendering SVM a more flexible PWM strategy compared to CBPWM techniques with rigid switching patterns [57], [58], [59], [60]. Moreover, during a switching period, the choice of null voltage vectors, e.g. 000 and 111, is also available in SVM, which is often utilized to optimize switching losses, harmonic performance, or balance losses, offering more flexibilities [61], [62]. Despite numerous variations, the seven-segment switching sequence SVM predominates in various applications, including motor drives, compared to other alternative SVM techniques with different switching sequences. This study considers the seven-segment SVM for comparison with other PWM techniques.

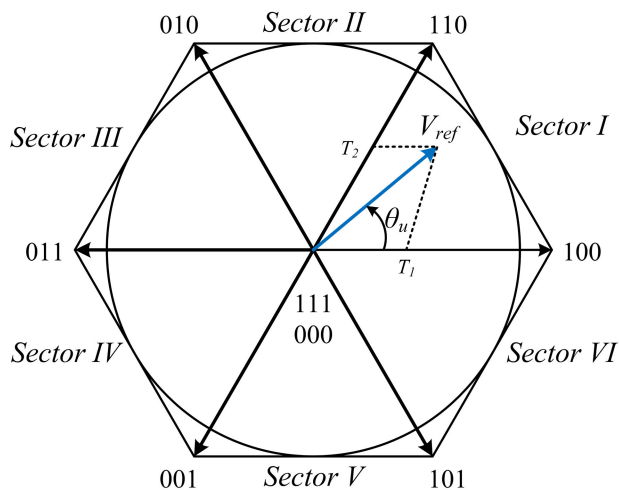


FIGURE 5. Space vector representation of the eight switching states of 2L-VSIs in the $\alpha\beta$ frame.

C. PRE-PROGRAMMED PULSE WIDTH MODULATION

Pre-programmed PWM techniques generate switching signals by comparing pre-determined switching angles α_x , where $x \in \{1, 2, \dots, N\}$, with the reference voltage angle θ_u , as depicted in Fig. 6. Due to the pre-determined number of switching actions within a fundamental period of the inverter output voltage, the switching frequency of the pre-programmed PWM technique is synchronized with the

fundamental frequency. Consequently, this PWM technique is also widely referred to as synchronous optimal PWM (SOPWM) [63]. The switching angles for a given N number of switching actions are calculated offline over a quarter, half, or whole fundamental period based on the Fourier decomposition of the inverter output voltage waveform using various optimization algorithms [64], [65], [66].

The switching angles of pre-programmed PWM are optimized to achieve desired performance objectives. The optimization criteria for the switching angles can be categorized into selective harmonic elimination (SHE), which targets the elimination of lower-order harmonics in the output current, and SHM, which selectively minimizes harmonics within the desired harmonic range [67], [68], [69], [70]. Particularly, SHM is widely used in various applications as it allows mitigation of a broad range of harmonics. The primary optimization objectives of SHM include mitigation of current harmonics [71], [72], switching loss [73], torque ripple [74], DC-link current ripple [75], and multi-performance objectives [76].

After being optimized, the switching angles are stored in the memory of microcontrollers as look-up tables (LUTs) to generate PWM signals in real-time [77]. However, in recent years, real-time optimization of the switching angles has become feasible thanks to the increased computational capability of digital controllers and the introduction of efficient optimization algorithms and artificial neural networks (ANNs). Subsequently, numerous researchers have focused on the real-time calculation of the switching angles [78], [79], [80], [81]. In this approach, the switching angles are continuously computed online, eliminating the need for large memory space to store the pre-calculated switching angles at the expense of the increased computational burden. These online SHE and SHM methods offer significant advantages over their standard counterparts that rely on offline optimization. They are more adaptable to changes in operating conditions and enable faster control dynamics, provided that the microcontroller can handle the additional computational burden imposed by the online optimization algorithms.

Compared to other PWM techniques, the pre-programmed PWM techniques offer significantly lower THD, thanks to the optimized switching angles, making them a preferred modulation strategy for high-power and high-speed applications where the switching-to-fundamental frequency ratio m_f is usually lower [82]. These PWM techniques are widely used in medium-voltage, high-power multilevel VSIs where minimizing switching loss is of utmost importance [83], [84]. However, in the context of 2L-VSIs, pre-programmed PWMs are often employed in higher-speed regions of motor drives to extend the operational range of the motor, as these techniques can maximize DC-link voltage utilization while maintaining good harmonic performance without experiencing an increase in lower-order harmonics at lower switching-to-fundamental frequency ratios [85], [86].

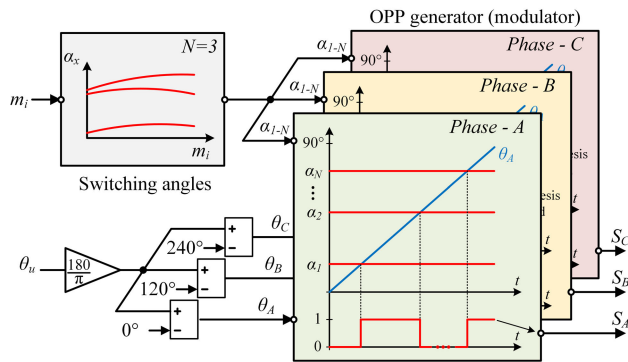


FIGURE 6. The principle of pre-programmed PWM technique.

D. HYSTERESIS PULSE WIDTH MODULATION

The hysteresis PWM technique generates switching signals by comparing the measured output current of the VSI with pre-defined bands around the reference signal, as illustrated in Fig. 7. When the phase current surpasses the upper band, the hysteresis control turns off the upper switch and turns on the lower switch of the corresponding phase. Conversely, when the current falls below the lower boundary, it turns on the upper switch and off the lower switch. Consequently, the output current of the VSI oscillates within the hysteresis band. However, in the case of three-phase inverters, the direction of phase currents is dictated by the switching states of all three phases. Therefore, controlling the switching states of each phase individually results in current overflow from the pre-defined hysteresis band, as shown in Fig. 7. To mitigate this issue, the hysteresis PWM technique is preferred for high switching frequency conditions [32].

Although this PWM technique offers excellent dynamic performance and does not require prior knowledge of the load parameters during the implementation, its switching frequency significantly fluctuates depending on the load impedance, even when the hysteresis bandwidth and operating points remain constant. This variability leads to highly uncharacteristic harmonic performance, drastically impacting the efficiency of the VSIs [87], [88]. Due to these limitations, hysteresis PWM has fallen out of favor among VSIs. Moreover, compared to other PWM techniques, hysteresis PWM requires current sensors to generate PWM signals. These drawbacks have gradually restricted the applicability of the hysteresis PWM for many applications, such as motor drives and high-power converters [89]. Consequently, this method is seldom employed in VSIs nowadays. Therefore, the hysteresis PWM is excluded from the comparison.

V. COMPARATIVE ANALYSIS

The performance of commonly used PWM techniques from each category in Fig. 2, including SPWM, ZSI-PWM, THI-PWM with a gain of 1/4, SVM, and SHM with up to 100th order non-triplen odd WTHD minimization, presented in [90], has been evaluated side-by-side in terms of their

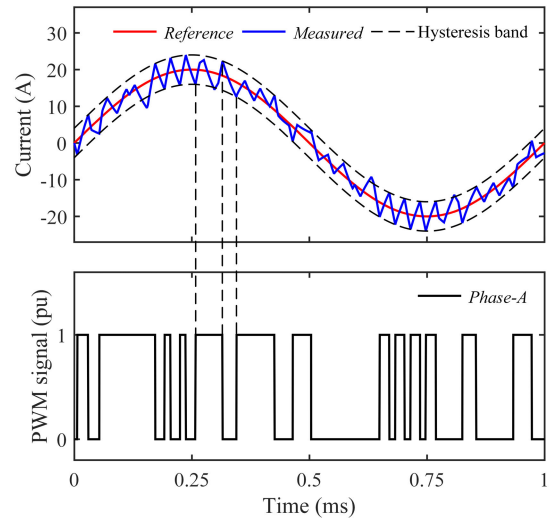


FIGURE 7. The principle of hysteresis PWM technique.

harmonic performances and DC-link voltage utilization. This evaluation was carried out on an experimental setup equipped with a rapid prototyping PLECS RT-Box3 and a 2L-VSI with silicon carbide (SiC) MOSFETs, connected to a three-phase RL-load, as shown in Fig. 8. During the experiments, the user selects the desired PWM technique and its operating conditions in PLECS RT-Box3 through the host-PC. Then, the RT-Box3 generates the PWM signals in real-time, which are applied to the 2L-VSI. While the 2L-VSI is operating, the output voltage and current waveforms are recorded using digital oscilloscopes to analyze the harmonic performance and DC-link utilization. The remaining performance indices are discussed based on the findings of the literature. The experimental conditions and parameters are summarized in Table 1.

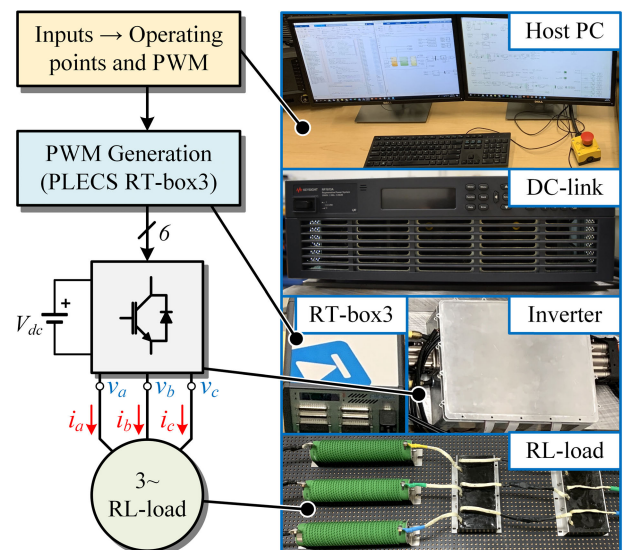


FIGURE 8. The experimental setup.

TABLE 1. Parameters and experiment conditions.

Parameters	Symbol	Value
DC-link voltage	V_{dc}	50 V
Resistive load	R	1 Ω
Inductive load	L	512 μ H
Fundamental frequency	f_l	60 Hz
Switching-to-fundamental frequency ratio	m_f	5 – 29
Deadtime	T_d	300 ns
Switching freq.	f_{sw}	0.3-1.74 kHz

A. HARMONIC PERFORMANCE

This subsection comprehensively analyzes the harmonic performance of the aforementioned PWM techniques within their linear operating range. Furthermore, the relation between harmonic performance, modulation index and switching frequency are exhibited.

Fig. 9 illustrates the relationship between harmonic performance and output voltage at a switching-to-fundamental frequency ratio of 15. As the modulation index increases, current harmonics decrease in all PWM techniques, indicating a similar inverse relation to modulation indexes. However, for the pre-programmed PWM technique, current distortion increases when modulation indexes exceed 1.2. At higher modulation indexes, the pulse patterns produced by SHM become closer to the six-step pattern as it approaches the six-step operation. Thus, $d = 1$ is expected at the maximum modulation index of $4/\pi$. Moreover, it is essential to note that the harmonic performance of the PWM techniques varies differently depending on the switching-to-fundamental frequency ratio. Therefore, the results in Fig. 9 should only be used to observe the relationship between harmonic performance and modulation index.

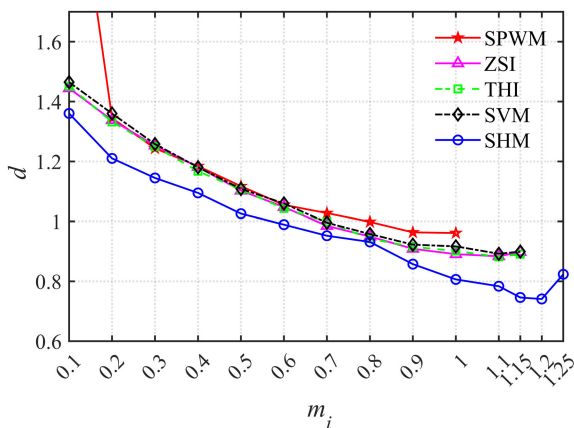


FIGURE 9. Relationship between current distortion factor and modulation index at $m_f = 15$.

Fig. 10 presents the relationship between harmonic performance and the switching-to-fundamental frequency

ratio. The results clearly indicate that all PWM techniques offer better harmonic performance at higher switching-to-fundamental frequency ratios, highlighting an inevitable trade-off between switching loss and current distortion. However, as the switching-to-fundamental frequency ratio increases, the effectiveness of the SHM diminishes, resulting in nearly the same current distortion as other PWM techniques. Consequently, choosing the pre-programmed PWM technique becomes less desirable when the switching-to-fundamental frequency ratio exceeds twenty-one, i.e., $m_f > 21$. Conversely, it exhibits significantly better harmonic performance at lower switching-to-fundamental frequency. Therefore, pre-programmed PWM techniques are more suitable for lower switching-to-fundamental frequency conditions, while other PWM techniques are more appropriate for higher switching-to-fundamental frequency conditions.

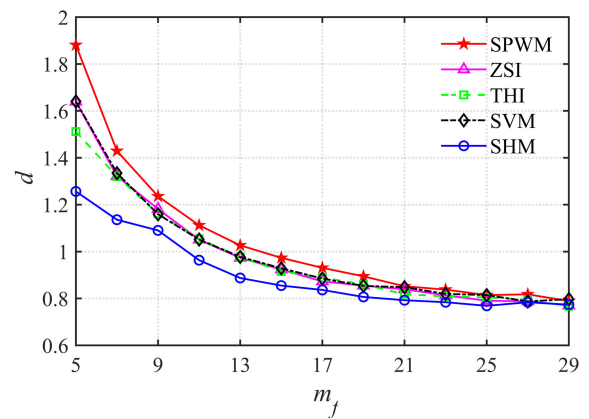


FIGURE 10. Relationship between current distortion factor and switching frequency with respect to fundamental frequency at $m_i = 0.9$.

Fig. 11 illustrates the harmonic spectrums of the phase currents produced by the PWM techniques. Although the amplitude of the harmonics depends on the load impedance, the trend and harmonic characteristics of each PWM technique can be observed in detail.

SHM demonstrates significantly lower THD than other PWM techniques, primarily due to its pre-optimized switching angles to minimize harmonic components for a given set of switching actions. Furthermore, the pre-programmed PWM techniques do not produce large harmonics around the switching frequency as their switching patterns do not feature symmetric switching cycles like CBPWM techniques. Thereby, specific order harmonics components, especially lower-order harmonics, can be mitigated regardless of the switching-to-fundamental frequency ratio, offering more flexible harmonic characteristics. However, in pre-programmed PWM, the harmonic spectrum shifts relative to the fundamental frequency as the switching frequency is synchronized with the fundamental frequency.

On the contrary, other PWM techniques are mainly employed with fixed switching frequencies and feature symmetric switching cycles due to the fixed carrier waveform, resulting in significant harmonics around multiple integers of the switching frequency when operating in their linear region. However, the harmonic quality is evaluated with respect to the fundamental frequency of the inverter. Therefore, the dominant harmonics are represented by multiples of the switching-to-fundamental frequency ratio. This suggests that the dominant harmonics produced by SVM and CBPWM techniques have a direct linear relationship with the switching-to-fundamental frequency ratio. Therefore, large lower-order harmonic components become inevitable at lower switching-to-fundamental frequency ratios. This is an undesirable scenario for VSIs, especially those used in motor drive applications where torque ripples generated by lower-order harmonics cannot be effectively damped out by mechanical inertia [91], [92].

Moreover, in SVM and CBPWM techniques, the switching-to-fundamental frequency ratio might not always be an integer when a fixed switching frequency is utilized due to the variable fundamental frequency, leading to the production of subharmonics. Especially when the ratio between the switching and fundamental frequencies is low, large low-order subharmonics are produced, drastically deteriorating the harmonic performance. As a result, these PWM techniques are best suited for higher switching-to-fundamental frequency ratio conditions [93].

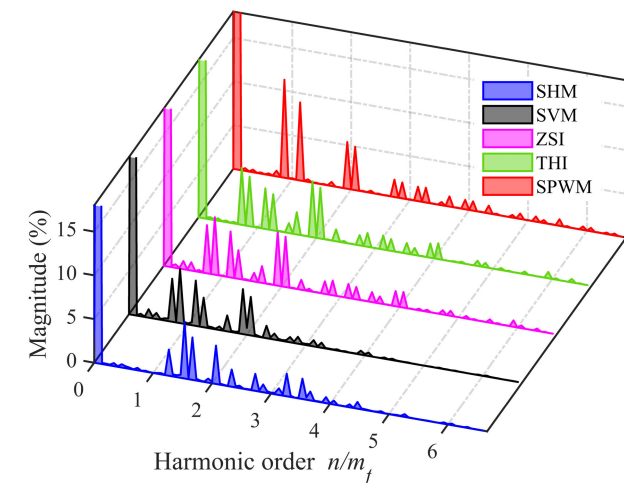


FIGURE 11. Spectrum of the phase current harmonic components respect to fundamental components at $m_i = 0.9$ and $m_f = 15$.

As shown in Figs. 9-11, it is evident that SVM, ZSI-PWM, and THI-PWM showcase similar harmonic performances. Therefore, SVM was chosen to represent the harmonic performances of these three PWM techniques in Figs. 12 and 13.

Fig. 12 compares the current distortion factors of each PWM technique operating under various conditions. A wide

range of switching-to-fundamental frequency ratios was selected to ensure a fair comparison, along with their linear modulation index range starting from a modulation index of 0.1. The harmonic performance trend observed in Figs. 9 and 10 remained consistent.

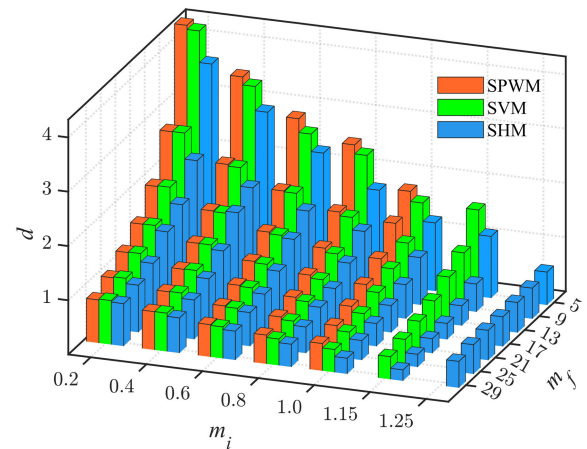


FIGURE 12. Comparison of current distortion for commonly used PWM techniques.

Fig. 13 illustrates the performance of the PWM techniques in terms of WTHD. As expected, the WTHD shows a similar trend to the current distortion factor in Fig. 12. However, at lower switching-to-fundamental frequency ratios, there is a noticeable increase in the WTHD at the maximum modulation indexes of SPWM and SVM due to very short pulses at maximum modulation index.

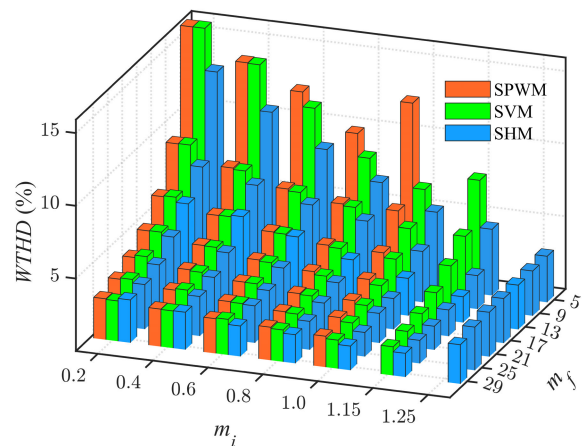


FIGURE 13. Comparison of WTHD for commonly used PWM techniques.

Based on the harmonic analyses presented above, it is evident that the output power quality of the PWM techniques is inversely correlated with their switching frequency. However, as explained in Section III-A, increasing the switching frequency leads to higher switching losses due to more frequent switching events of semiconductors, which

ultimately results in reduced VSI efficiency and power density.

Fig. 14 shows the comparative switching loss analysis for SPWM, SVM, and SHM as a function of the current distortion factor, with SVM representing ZSI-PWM, THI-PWM, and SVM itself as they exhibited similar performance characteristics. To clearly illustrate the PWM-associated switching losses, this analysis was carried out in the PLECS simulation environment under identical conditions to the experimental validation, using manufacturer-provided semiconductor loss data [94]. The results clearly demonstrate the trade-off between the output power quality and switching losses. SHM exhibited the least switching losses compared to the other PWM techniques, as it delivers the same harmonic performance at a much lower switching frequency. Meanwhile, SVM consistently offers lower switching losses than SPWM, thanks to its improved harmonic performance. In this analysis, the switching losses are normalized by the maximum switching loss of SPWM.

In conclusion, it can be observed that PWM techniques with good harmonic performance directly contribute to the reduction of switching losses, as a lower switching frequency can be selected to achieve the same power quality.

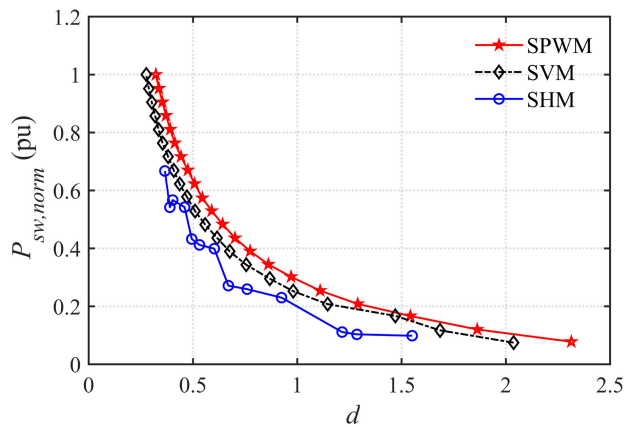


FIGURE 14. Relationship between switching loss and current distortion factor at $m_i = 0.9$.

B. DC-LINK VOLTAGE UTILIZATION

The DC-link voltage utilization of the SPWM, SVM, and SHM was investigated at a switching-to-fundamental frequency ratio of 21. It is important to note that the performance of ZSI-PWM and THI-PWM provided similar performance to SVM. Thus, for simplicity, they are also represented by SVM in this analysis. As mentioned in subsection IV-A, the amplitude ratio of the modulating signal to the carrier waveform is termed as the reference modulation index $m_i^* = V_{x,peak}^*/V_{carrier}$, while the amplitude ratio of the output voltage fundamental component to half of the input DC-link voltage is termed as $m_i = V_1/(V_{dc}/2)$, as given in (6). Fig. 15 illustrates the output modulation index as a

function of the reference modulation index for each PWM technique.

As shown in Fig. 15, SPWM preserves the same ratio between the reference and output modulation indexes until the reference modulation index exceeds 1. On the other hand, SVM, ZSI-PWM, and THI-PWM produce $\sim 2/\sqrt{3}$ higher output modulation index for a given reference modulation index due to their resultant modulating signals, which feature wider voltage waveforms with smaller amplitudes than sinusoidal modulating signals, such as those in SPWM. This results in an approximately 15% extended linear modulation range, effectively improving the DC-link utilization rate of VSIs. However, these PWM techniques reach the maximum point of their linear operation range before reaching the six-step operation (square wave) and exhibit nonlinearity above the extended linear range. In the overmodulation region, where the reference modulation index is greater than 1, the linear relationship between the output voltage and modulating signal no longer exists. Moreover, operating in nonlinear regions is highly undesirable as these PWM techniques produce significant lower-order harmonics and lose the harmonic characteristics outlined in the harmonic performance section. This occurs due to reduced switching frequency as the amplitude of modulating signals becomes larger than the carrier waveform. As a result, these PWM techniques are rarely used in their nonlinear region without employing an additional overmodulation scheme to ensure acceptable performance.

It is also important to emphasize that, in Fig. 15, the reference modulation index is defined as the amplitude ratio of the modulating signal to the carrier signal rather than the fundamental components, to represent the linear range. In other words, in SVM, ZSI-PWM, and THI-PWM techniques, the fundamental components of the reference and output voltage remain equivalent up to the output modulation index value of 1.155, which corresponds to an extended DC-link utilization range from $V_{dc}/2$ to $V_{dc}/\sqrt{3}$, thanks to their resultant modulating waveforms with lower amplitude but with the same fundamental component. In practical implementation, the reference modulation index for these PWM techniques is typically calculated based on the fundamental component of the reference voltage vector prior to generating the resultant modulating signals, e.g., before injecting a third harmonic, and is then multiplied by $\sqrt{3}/2$ to represent the linear range from 0-1.

While the other PWM techniques have limited linear range, the SHM exhibited a linear operation range up to the six-step operation, representing the maximum possible DC-link voltage utilization of 2L-VSIs. This is feasible in the pre-programmed PWM techniques as their switching angles are typically optimized over the entire modulation index range. Thus, the pre-programmed PWM techniques can achieve both excellent harmonic performance and maximum DC-link utilization, making them ideal PWM techniques for high-speed motor drives where higher DC-link utilization and low THD are essential.

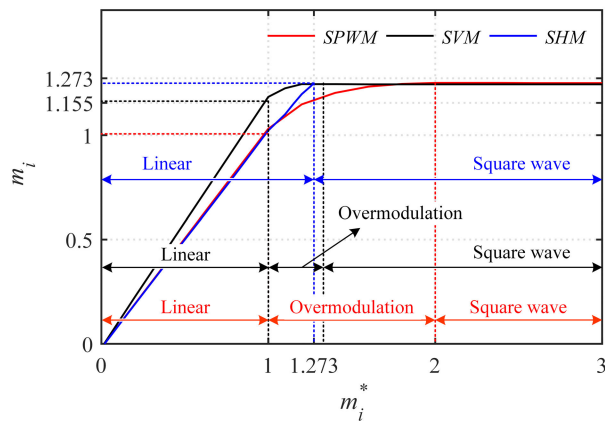


FIGURE 15. Comparison of DC-link utilization of the commonly used PWM techniques at $m_f = 21$.

C. DYNAMIC PERFORMANCE

In open-loop systems, the dynamic response of PWM techniques is directly tied to their switching frequencies. Faster dynamic responses are anticipated at higher switching frequencies as the output voltages update more frequently. However, the maximum switching frequency of the employed PWM techniques is limited by inherent constraints of the semiconductor switching devices, switching losses, and the delay between the sampling/interrupt and PWM update in the digital controller [95], [96].

In closed-loop systems, the dynamic performance of the VSIs is dictated by the bandwidth of the closed-loop control, which has a much lower bandwidth than the switching frequency [46]. Depending on the implementation and the type of PWM used, the bandwidth and structure of closed-loop control are adjusted to accommodate the PWM technique. The dynamic performance of each type of PWM technique is discussed individually:

1) CBPWM TECHNIQUES

Apart from the switching frequency, in digital implementations with naturally sampled conditions, the dynamic performance of PWM techniques is limited by the control frequency of the digital controller, which is equivalent to the reference update rate [97]. Thus, reducing the computational burden on the controller would aid in achieving faster dynamic performance, a key advantage of CBPWM techniques. Furthermore, their disturbance-free carrier waveforms make CBPWM techniques less sensitive to modulating signal noise than other PWM techniques despite their poor harmonic performance. This enables them to function with closed-loop control with higher bandwidth, implying higher dynamic performance capability. Moreover, CBPWM techniques are typically utilized at higher switching-to-fundamental frequency ratio conditions [93]. Hence, it is expected that the dynamic performance of CBPWM techniques is to be high.

2) SVM

SVM demonstrates dynamic performance similar to CBPWM techniques since they are commonly employed under similar switching-to-fundamental frequency ratio conditions. However, in comparison to CBPWM techniques, the output waveform quality of SVM is more susceptible to disturbances in the modulating signal. This sensitivity arises due to complex mathematical operations involved in forming the switching signals based on the reference voltage vector, which is directly calculated from the modulating signals, which contain disturbances [98]. Additionally, compared to CBPWM techniques, SVM introduces a more significant real-time computation delay between sampling and processing, contributing to phase delay in control and harmonic performances [99]. Consequently, the bandwidth of closed-loop controls may need to be reduced to avoid compromising SVM performance.

3) PRE-PROGRAMMED PWM

It is widely acknowledged that pre-programmed PWM techniques suffer from poor dynamic performance owing to their extreme sensitivity to the noise in the magnitude and angle of the modulating signal [100]. In closed-loop control methods such as conventional field-oriented control (FOC), ripples in the modulating signal typically arise from harmonic components in the feedback current, PI regulators and measurements noise [101]. This ripple in modulating signal magnitude leads to continuous changes in the pre-defined switching angles, which are calculated as a function of the modulation index, resulting in deviations from the ideal switching angles [102]. The optimal performance of pre-programmed PWM techniques is highly reliant on precise switching, and any deviation from the pre-defined switching angles can significantly degrade harmonic performance [103]. Moreover, the pre-defined switching angles often include discontinuities, leading to abrupt changes in the switching states when the modulation index passes over these discontinuities [104].

In contrast to other PWM techniques, where switching signals are generated by comparing modulating signals with noise-free carrier waveforms, pre-programmed PWM techniques generate switching signals by comparing the pre-defined switching angles with the reference voltage angle derived from the modulating signals, which contain noise and deviations when used in closed-loop systems. Due to the closed-loop behavior and disturbances, the reference voltage angle often fluctuates, resulting in unnecessary excessive switching actions as it repeatedly crosses over the pre-defined switching angles instead of crossing over once per period [105]. Therefore, pre-programmed PWM techniques exhibit a significant drop in performance in closed-loop systems and cannot operate within typical control bandwidth, as a higher bandwidth leads to a noisier modulating index and reference voltage angle.

As a result, pre-programmed PWM techniques require low bandwidth in closed-loop systems to achieve optimal performance under steady-state conditions when conventional linear closed-loop controls are employed [106]. However, this reduction in bandwidth significantly compromises the dynamic response of the closed-loop system. Nonetheless, to accommodate pre-programmed PWM techniques, state-of-the-art stator flux tracking and model predictive pulse pattern (MP³C) methods have been developed to achieve fast dynamic performance in industrial motor drives, although with a trade-off of increased complexity and computational burden [107], [108].

D. COMPLEXITY

1) CBPWM TECHNIQUES

CBPWM techniques have the least hardware requirements due to their straightforward approach to generating the switching signals. Nowadays, most DSPs come equipped with dedicated high-performance PWM peripherals tailored for CBPWM techniques. In these peripherals, the modulating signals are compared with a high-resolution triangular waveform to generate the switching signals in real-time [109]. Additionally, CBPWM techniques are typically utilized with fixed switching frequencies. Therefore, a simple regular sampling method can be easily implemented in digital implementation, where the measurements are updated at the minimum and maximum points of the triangular waveform [110]. This sampling approach enables the measurement of the average current while avoiding current ripples and commutation noises. This drastically simplifies the closed-loop implementation process, although with a minor trade-off of a small delay between control updates and sampling, which can be effectively compensated [111]. Moreover, CBPWM techniques offer various sampling methods, enhancing their feasibility across different hardware platforms [112], [113].

2) SVM

SVM relies on several mathematical operations for real-time calculations of dwell times and switching sequences in real-time, which requires more microprocessor processing capabilities [99], [114]. Nevertheless, SVM does not encounter challenges similar to those faced by pre-programmed PWM techniques. PWM strategies derived from SVM, such as ZSI-PWM and discontinuous PWMs, can be implemented based on CBPWM methods where modulating signals are formed by adding the calculated voltage vectors instead of generating the switching sequence directly [115], [116]. Consequently, even analog implementations of SVM are becoming feasible, offering multiple approaches during implementation [40]. In terms of sampling, SVM can be synchronized with the switching frequency based on counters, as it is commonly implemented with a fixed switching frequency. Furthermore, in CBPWM-based implementations, SVM can also utilize the same sampling approaches as the CBPWM techniques, further extending its sampling capabilities.

3) PRE-PROGRAMMED

Despite its straightforward implementation process, pre-programmed PWM introduced complexity to the closed-loop control system for the following reasons:

- 1) *Optimization and discontinuities*: Although the calculation of optimal switching angles is an offline procedure, it requires knowledge of Fourier decomposition series and nonlinear optimization methods as this process involves solving nonlinear transcendental equations [117]. Moreover, the globally optimum switching angles may contain discontinuities over a broader modulation index [118]. These discontinuities introduce interpolation errors, unnecessary switching actions, and increased current ripple [119], [120]. Consequently, integrating pre-programmed PWM with conventional closed-loop controls is challenging without employing complex closed-loop control or post-optimization processes for continuous switching angles across the modulation index range or hysteresis band range [121], [122].
- 2) *Sampling*: Pre-programmed PWM techniques require hardware with several MHz control frequency capabilities, such as a field programmable gate array (FPGA), to generate switching signals close to optimal switching angles [123], [124]. Moreover, unlike other PWM techniques, pre-programmed PWM techniques use a natural sampling method due to the lack of fixed time intervals between the switching actions to trigger sampling instants. This results in the acquisition of both fundamental components and phase current ripples in closed-loop control [125]. Consequently, the closed-loop control attempts to correct current ripples, leading to significant noise injection into the modulating signals and worsening harmonic performance [126]. Addressing this issue often involves employing fundamental current estimation, complex observers, and change of closed-loop controls [127], [128].
- 3) *Smooth transition*: In motor drive applications, the fundamental frequency of VSIs can vary widely [129]. Therefore, several sets of switching angles with different switching-to-fundamental frequency ratios are employed to maintain the switching frequency within the desired range and achieve good THD performance across a wide speed range [130]. However, transitioning between different sets of switching angles leads to undesired large current oscillations and transient effects on the load [131]. To mitigate this issue, smooth transition schemes need to be included in variable switching frequency schemes, further increasing the complexity of pre-programmed PWM techniques [85], [132]. Additionally, employing a large number of different sets of switching angles with high accuracy drastically increases the memory space requirements for the hardware [103]. Consequently, the cost of

control platforms used in pre-programmed PWM techniques is typically high.

E. SUMMARY

This subsection offers a comprehensive side-by-side comparison of the PWM techniques based on the discussed performance criteria, as shown in Fig. 16. Complexity is categorized into flexibility and hardware requirements, recognizing that the complexity of PWM techniques varies depending on implementation approaches. Moreover, the harmonic performance is divided into switching loss and THD performance since delivering low THD at a lower switching-to-fundamental frequency ratio directly enables VSI to reduce switching frequency, thereby reducing switching losses. In addition to the performance comparison, table 2 summarizes the main advantages, disadvantages, and primary application areas of PWM techniques.

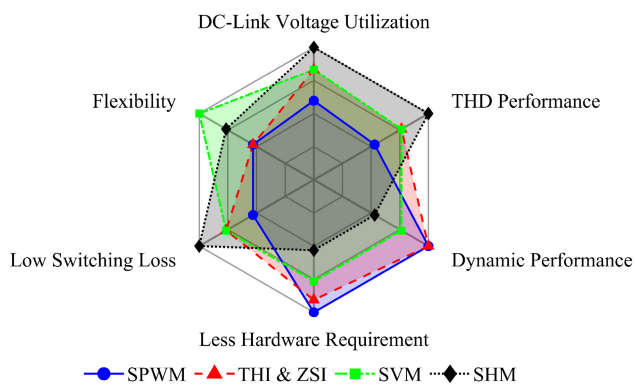


FIGURE 16. Summary of the commonly used PWM techniques.

VI. FUTURE TRENDS

This section explores the future trends in PWM techniques, focusing on their potential application areas and evolving requirements. It discusses the impact of digital controllers, wide-bandgap (WBG) semiconductors, and MPC on PWM techniques in 2L-VSIs. Additionally, it also provides a brief outlook on the future of PWM techniques for multiphase 2L-VSIs—those with more than three phases—which have garnered significant interest in recent years.

A. TRENDS OF PWM TECHNIQUES

With the global effort to reduce carbon dioxide (CO₂) emissions, there has been a significant surge in demand for electrified vehicles [133]. While most developments have centered around passenger electric vehicles, the range of electrified vehicles is rapidly expanding, imposing new and broader requirements on VSIs, such as broader operation ranges, reduced switching losses, higher power density, and improved power quality [134]. However, there is no single PWM technique that can fulfill these requirements across all operating points. To address this challenge, various research works are exploring the combination of

different PWM techniques [132], [135], [136]. In these approaches, different PWM techniques are employed under specific operating conditions where they exhibit their optimal performance, leveraging the advantages of multiple PWM techniques to achieve improved performance across the entire operation range, thus resulting in a hybrid PWM technique [137]. However, implementing multiple PWM techniques increases control and hardware complexity, as each modulation scheme has distinct requirements for generating switching signals. Subsequently, hybrid PWM requires a flexible controller architecture and well-designed smooth transition logic between PWM modes to prevent output discontinuities or instability [85]. This results in increased computational demand and complexity. Nevertheless, with ongoing advancements in DSPs and FPGAs, such implementations are becoming increasingly practical for real-world applications.

With the growing advancement of artificial intelligence (AI) techniques such as ANNs, AI-driven methods have been explored to enhance or replace conventional PWM techniques [79], [80]. These AI-based approaches offer promising performance improvements, including fast dynamic response, better adaptability, and good steady-state performance. However, these benefits come at the cost of high computational requirements, increased complexity, the need for extensive data for offline model training, and a lack of predictable performance under extreme or unusual operating conditions. Despite these challenges, AI-assisted PWM techniques could offer a practical pathway toward real-world integration by leveraging AI algorithms to enhance the performance of traditional PWM techniques while preserving their safety and stability features, striking a balance between performance and reliability. As computational hardware becomes more powerful and affordable, and as standardized validation frameworks for AI-based control continue to mature, such techniques are expected to play a significant role in next-generation power electronic systems.

B. NEW REQUIREMENTS OF PWM TECHNIQUES

Due to PWM-controlled discrete output voltage waveforms, VSIs generate significant current ripples on the DC-link voltage. These current ripples are mitigated by using DC-link capacitors to stabilize the DC-link voltage, making them one of the main components in VSIs [138]. Compared to other components like semiconductor switching devices, the sizing of the DC-link capacitors is highly dependent on the switching frequency of the VSI. Traditionally, it has been expected that the size of capacitors would increase when VSIs are designed to operate at lower switching frequencies [139]. However, several studies have been conducted to derive analytical expressions for current ripples and harmonic components in DC-link capacitors produced by PWM signals [140], [141], [142]. This opens up the possibility for PWM techniques typically employed at low

TABLE 2. Summary of the commonly used PWM techniques.

PWM techniques	Advantages	Disadvantages	Primary applications
SPWM	<ul style="list-style-type: none"> ▪ Simplicity ▪ Lower hardware requirements 	<ul style="list-style-type: none"> ▪ Low DC-link voltage utilization ▪ Higher THD than the other methods 	<ul style="list-style-type: none"> ▪ Large variety of applications: grid, PV system, UPS, motor drives, etc. ▪ Low power drives ▪ Low-medium speed region
SVM	<ul style="list-style-type: none"> ▪ Improved THD performance ▪ Higher DC-link voltage utilization ▪ Flexibility 	<ul style="list-style-type: none"> ▪ Complexity ▪ Higher computational requirements 	<ul style="list-style-type: none"> ▪ Wide range of applications ▪ Electric vehicles
ZSI	<ul style="list-style-type: none"> ▪ Higher DC-link voltage utilization ▪ Same THD as seven-segment SVM ▪ Simpler than SVM 	<ul style="list-style-type: none"> ▪ Rigid switching sequence ▪ High common mode voltage production 	<ul style="list-style-type: none"> ▪ Wide range of applications ▪ Motor drives
THI	<ul style="list-style-type: none"> ▪ Less common mode voltage ▪ Slightly better THD than ZSI-PWM 	<ul style="list-style-type: none"> ▪ Complex calculation of 3rd harmonic in closed loop ▪ Slightly lower DC-link voltage utilization than ZSI-PWM 	<ul style="list-style-type: none"> ▪ Common mode voltage reduction
SHM	<ul style="list-style-type: none"> ▪ Maximum DC-link voltage utilization ▪ Good THD performance ▪ Less switching loss ▪ Different cost functions 	<ul style="list-style-type: none"> ▪ High hardware requirement, i.e. high memory space consumption, higher sampling frequency ▪ Not suitable for the higher switching-to-fundamental frequency ratio ▪ Poor dynamic performance 	<ul style="list-style-type: none"> ▪ High power drives ▪ High-speed region ▪ Railway ▪ Grid converters

switching frequency conditions, such as pre-programmed PWM techniques, to mitigate DC-link capacitor current ripple [143]. By considering this ripple during the offline switching angles calculations, along with load side output current harmonic, the size and cost of the capacitors can be reduced, achieving higher power density even at low switching frequency operation by merely modifying the PWM signals. Given the general demand for high-power density and low cost in VSIs, the minimization of the DC-link capacitor current ripple must be considered a critical requirement for PWM techniques.

Considering the increased voltage requirements and rapid development of fast-switching semiconductors, common-mode voltage is becoming a more significant issue [144]. Thus, common mode voltage should be considered to reduce the risk of bearing faults in motor drive applications [145], [146], imposing new requirements on PWM techniques.

C. DIGITAL CONTROLLERS

Digital implementation of PWM techniques predominates in modern power converters, thanks to advances in digital controllers such as microcontrollers (MCs), DSPs, and FPGAs [147]. These programmable digital controllers offer various advantages, including simplified control circuitry, reduced size, flexibility, and easy reprogramming. In addition to these advantages, various control strategies for VSIs can be implemented in the digital controller, along with PWM techniques [148], [149]. Despite their advantages, the performance of digital controllers is continuously improving,

favoring the widespread adoption of more complex and performance-oriented PWM techniques, such as hybrid PWM in motor drive applications [90].

However, several studies have reported using combined digital controllers, such as DSP+FPGA, to achieve better performance in SVM and hybrid PWM techniques [123], [150]. This trend suggests that the demand for high-performance digital controllers for more complex PWM techniques still exists.

D. POWER SEMICONDUCTORS

Nowadays, the use of WBG semiconductor switching devices, such as SiC and gallium nitride (GaN), in PWM-controlled VSIs is becoming more common due to their high-temperature tolerance and fast switching capabilities [151], [152]. With the introduction of WBG semiconductors, VSIs can operate at much higher switching frequencies, reducing the significance of harmonic performance in PWM techniques, as they typically provide better harmonic performance at higher switching frequencies. Moreover, due to the fast switching of WBG devices, deadtime can be significantly reduced, further mitigating the adverse effects of deadtime on harmonic performance. Consequently, the importance of deadtime and inverter nonlinearity compensation methods decreases due to the reduced delay between PWM signals at the gate drivers and actual voltage patterns [153].

In addition to enhancing harmonic performance, WBG semiconductors enable better dynamic performance in

commonly used regular sampled PWM techniques, as the control frequency of digital controllers can be increased along with the switching frequency, which is usually limited to one or two times the maximum switching frequency of the semiconductor switching device. It can be concluded that WBG semiconductor switching devices lower the harmonic and dynamic performance requirements of PWM techniques due to the increased switching frequency. However, WBG semiconductor-based VSIs still face challenges such as high prices, significant electromagnetic interference (EMI), and voltage oscillations that negatively affect the load insulation [154], [155], [156], [157]. These issues must be carefully considered during the selection of the PWM technique.

E. MODEL PREDICTIVE CONTROL

In recent years, the advancement of digital controllers has made it possible to implement more computationally demanding strategies, such as the finite control set model predictive control (FCS-MPC) to control VSIs in motor drives [158], [159], [160]. Short horizon FCS-MPC (SH-FCS-MPC), characterized by its straightforward design and excellent dynamic performance, directly considers the switching states in the control structure, eliminating the need for a modulator [161]. However, challenges such as the inability to produce a fixed-switching frequency and elevated harmonic distortion have delayed its industrial adoption [162]. Conversely, long-horizon FCS-MPC (LH-FCS-MPC) offers enhanced closed-loop performance in both steady-state and transient conditions, lower harmonic distortion, and reduced switching losses at the expense of a more complex structure [163]. Despite its computational intensity and higher sampling frequency requirements, recent advances in FPGAs have significantly increased its feasibility [164]. Although LH-FCS-MPC can be a promising alternative to pre-programmed PWM techniques, some challenges remain, such as the inability to produce a fixed switching frequency and complex tuning requirements [162], [163].

Combining the optimal steady-state performance of pre-programmed PWM techniques, often referred to as optimized pulse pattern (OPP), with the fast dynamics of MPC, the MP³C offers a compelling solution [165]. MP³C uses the switching patterns of OPPs and modifies them in real-time to control the motor stator flux over a finite prediction horizon [108]. It is particularly suitable for medium-voltage drives and has already been found to be applicable in the industry [166]. MP³C delivers fast transient responses and maintains very low harmonic distortion levels per switching frequency during steady-state operating conditions [167]. However, during low-speed operation, FOC and SVM are necessary to obtain good performance [108]. Therefore, both FOC and SVM, as well as MP³C and OPPs, are required to be implemented in the same controller, increasing the computational requirements [168].

F. PWM TECHNIQUES FOR MULTIPHASE 2L-VSIs

In recent years, 2L-VSIs with more than three phases have gained significant interest in electrified transportation applications, such as electric vehicles and aircraft [169], [170]. Multiphase 2L-VSIs are commonly used with multiphase motors, which are well known for their fault tolerance, as these motors can operate even with one or more faulty phases [171], [172]. Additionally, multiphase 2L-VSIs can alleviate challenges associated with the paralleling of 2L-VSIs due to their inherent reduced current rating per phase [173]. Common phase numbers include 5-, 6-, 7-, 9-, and 11-phases. While higher phase count systems provide greater fault-tolerant capabilities, they increase the control complexity and component count [174].

PWM methods for multiphase 2L-VSIs generally fall into SPWM and SVM [175]. As in conventional three-phase 2L-VSIs, SPWM is known for its simplicity and ease of implementation, making it a widely used PWM technique for multiphase 2L-VSIs [176]. On the other hand, SVM optimizes switching sequences and exploits the redundancy in switching states to reduce current ripple and harmonic distortion [177]. Although SVM offers better DC-link utilization, SPWM can achieve similar results when combined with zero-sequence injection [178], [179]. Additionally, adapting SPWM for fault-tolerant operation is considerably simpler than SVM, which requires careful optimization of switching sequences for each fault scenario to maintain stability under fault conditions [180].

Although less explored, pre-programmed PWM techniques have already been extended for multiphase 2L-VSIs [181]. The optimization objectives of SHM can be adjusted depending on the phase configuration and type of load, making it particularly beneficial for multiphase motor drives [182]. Furthermore, its low harmonic advantage is amplified considering that the multiphase machines experience significant current harmonics at lower switching frequencies and lower modulation indices conditions, which can effectively be mitigated by SHM while maintaining a low switching frequency [183]. While the implementation and optimization objective of pre-programmed PWM may differ, it still entails the same advantages as it is in 2L-VSIs, such as better DC-link utilization and good harmonic performance. Given these benefits, pre-programmed PWM combined with advanced control methods, such as MPC, becomes a promising solution for multiphase 2L-VSIs [184].

VII. CONCLUSION

Classical PWM techniques remain widely employed in power converters despite the growing trend of advanced control strategies, such as MPC. This paper not only provides a detailed overview of the widely used PWM techniques in 2L-VSIs but also offers a thorough side-by-side performance comparison across a broader range of operating conditions. By meticulously examining the performance of each PWM

technique, this study serves as both a comprehensive introduction to PWM techniques and a valuable resource for readers to select the most suitable PWM technique for their specific application.

The presented comprehensive analysis reveals that CBPWM and SVM techniques demonstrate better performance when the switching-to-fundamental frequency ratio exceeds 21. Conversely, pre-programmed PWM techniques excel in scenarios with lower switching-to-fundamental frequency ratio conditions, which are commonly encountered in applications involving high-speed machines or high-power converters with low switching frequencies. Furthermore, as microcontrollers become more powerful and cost-effective, performance-oriented approaches such as MPC, AI-based methods, and hybrid PWM techniques will emerge as viable and attractive solutions for commercial 2L-VSIs.

REFERENCES

- [1] S. Kouro, J. Rodriguez, B. Wu, S. Bernet, and M. Perez, "Powering the future of industry: High-power adjustable speed drive topologies," *IEEE Ind. Appl. Mag.*, vol. 18, no. 4, pp. 26–39, Jul. 2012.
- [2] S. Kouro, M. Malinowski, K. Gopakumar, J. Pou, L. G. Franquelo, B. Wu, J. Rodriguez, M. A. Pérez, and J. I. Leon, "Recent advances and industrial applications of multilevel converters," *IEEE Trans. Ind. Electron.*, vol. 57, no. 8, pp. 2553–2580, Aug. 2010.
- [3] B. Wu and M. Narimani, *High-Power Converters and AC Drives*, 2nd ed., Hoboken, NJ, USA: Wiley, 2017.
- [4] S. Shuvo, E. Hossain, and Z. R. Khan, "Fixed point implementation of grid tied inverter in digital signal processing controller," *IEEE Access*, vol. 8, pp. 89215–89227, 2020.
- [5] N. Baekeland, D. Chatterjee, M. Lu, B. Johnson, and G.-S. Seo, "Overcurrent limiting in grid-forming inverters: A comprehensive review and discussion," *IEEE Trans. Power Electron.*, vol. 39, no. 11, pp. 14493–14517, Nov. 2024.
- [6] F. Blaabjerg, Y. Yang, K. A. Kim, and J. Rodriguez, "Power electronics technology for large-scale renewable energy generation," *Proc. IEEE*, vol. 111, no. 4, pp. 335–355, Apr. 2023.
- [7] P. Gonçalves, S. Cruz, and A. Mendes, "Finite control set model predictive control of six-phase asymmetrical machines—An overview," *Energies*, vol. 12, no. 24, p. 4693, Dec. 2019.
- [8] L. Chang, M. Alvi, W. Lee, J. Kim, and T. M. Jahns, "Efficiency optimization of PWM-induced power losses in traction drive systems with IPM machines using wide bandgap-based inverters," *IEEE Trans. Ind. Appl.*, vol. 58, no. 5, pp. 5635–5649, Sep. 2022.
- [9] Y. Shen, Z. Chen, H. Huang, Q. Wang, and Y. Liu, "Asymmetric space vector pulse width modulation for the phase current reconstruction in three-phase inverters," *IEEE Trans. Power Electron.*, vol. 40, no. 1, pp. 1686–1696, Jan. 2025.
- [10] B. Tamyurek, "A high-performance SPWM controller for three-phase UPS systems operating under highly nonlinear loads," *IEEE Trans. Power Electron.*, vol. 28, no. 8, pp. 3689–3701, Aug. 2013.
- [11] E.-K. Kim, F. Mwasilu, H. H. Choi, and J.-W. Jung, "An observer-based optimal voltage control scheme for three-phase UPS systems," *IEEE Trans. Ind. Electron.*, vol. 62, no. 4, pp. 2073–2081, Apr. 2015.
- [12] K. Zeb, W. Uddin, M. A. Khan, Z. Ali, M. U. Ali, N. Christofides, and H. J. Kim, "A comprehensive review on inverter topologies and control strategies for grid connected photovoltaic system," *Renew. Sustain. Energy Rev.*, vol. 94, pp. 1120–1141, Oct. 2018.
- [13] D. Kolantla, S. Mikkili, S. R. Pendem, and A. A. Desai, "Critical review on various inverter topologies for PV system architectures," *IET Renew. Power Gener.*, vol. 14, no. 17, pp. 3418–3438, Dec. 2020.
- [14] B. K. Gupta, K. R. Sekhar, and A. Kumar, "A novel multigain single-stage grid-connected inverter with asynchronous switching for intra-inverter circulating current elimination," *IEEE Trans. Power Electron.*, vol. 37, no. 12, pp. 15641–15653, Dec. 2022.
- [15] T. E. K. Zidane, A. S. Aziz, Y. Zahraoui, H. Kotb, K. M. AboRas, Kitmo, and Y. B. Jember, "Grid-connected solar PV power plants optimization: A review," *IEEE Access*, vol. 11, pp. 79588–79608, 2023.
- [16] A. VanderMeulen and J. Maurin. (2014). *Current Source Inverter Vs. Voltage Source Inverter Topology*. [Online]. Available: <https://www.eaton.com/content/dam/eaton/products/medium-voltage-power-distribution-control-systems/motor-control/literature/other-docs/sc9000-csi-vs-vsi-topology-white-paper-wp020001en.pdf>
- [17] H. W. van der Broeck, H.-C. Skudelny, and G. V. Stanke, "Analysis and realization of a pulsewidth modulator based on voltage space vectors," *IEEE Trans. Ind. Appl.*, vol. IP-24, no. 1, pp. 142–150, Jan. 1988.
- [18] A. M. Hava, R. J. Kerkman, and T. A. Lipo, "Simple analytical and graphical methods for carrier-based PWM-VSI drives," *IEEE Trans. Power Electron.*, vol. 14, no. 1, pp. 49–61, Jan. 1999.
- [19] G. Buja and G. Indri, "Improvement of pulse width modulation techniques," *Archiv für Elektrotechnik*, vol. 57, no. 5, pp. 281–289, Sep. 1975.
- [20] F. G. Turnbull, "Selected harmonic reduction in static D-C-A-C inverters," *IEEE Trans. Commun. Electron.*, vol. CE-83, no. 73, pp. 374–378, Jul. 1964.
- [21] G. S. Buja and G. B. Indri, "Optimal pulsewidth modulation for feeding AC motors," *IEEE Trans. Ind. Appl.*, vol. IA-13, no. 1, pp. 38–44, Jan. 1977.
- [22] J. Napoles, J. I. Leon, R. Portillo, L. G. Franquelo, and M. A. Aguirre, "Selective harmonic mitigation technique for high-power converters," *IEEE Trans. Ind. Electron.*, vol. 57, no. 7, pp. 2315–2323, Jul. 2010.
- [23] G. Nalcaci, D. Yildirim, I. Cadirci, and M. Ermis, "Selective harmonic elimination for variable frequency traction motor drives using Harris hawks optimization," *IEEE Trans. Ind. Appl.*, vol. 58, no. 4, pp. 4778–4791, Jul. 2022.
- [24] J. Holtz, "Pulsewidth modulation—A survey," *IEEE Trans. Ind. Electron.*, vol. 39, no. 5, pp. 410–420, Oct. 1992.
- [25] J. I. Leon, S. Kouro, L. G. Franquelo, J. Rodriguez, and B. Wu, "The essential role and the continuous evolution of modulation techniques for voltage-source inverters in the past, present, and future power electronics," *IEEE Trans. Ind. Electron.*, vol. 63, no. 5, pp. 2688–2701, May 2016.
- [26] H. Chen and H. Zhao, "Review on pulse-width modulation strategies for common-mode voltage reduction in three-phase voltage-source inverters," *IET Power Electron.*, vol. 9, no. 14, pp. 2611–2620, Nov. 2016.
- [27] A. Karuvaril Vijayan, D. Xiao, B. Nahid-Mobarakeh, and A. Emadi, "Synchronous optimal pulsewidth modulation for high-power AC motor drives: A review," *IEEE Trans. Transport. Electrific.*, vol. 10, no. 2, pp. 3976–3990, Jun. 2024.
- [28] J. Reimers, L. Dorn-Gomba, C. Mak, and A. Emadi, "Automotive traction inverters: Current status and future trends," *IEEE Trans. Veh. Technol.*, vol. 68, no. 4, pp. 3337–3350, Apr. 2019.
- [29] *IEEE Recommended Practice and Requirements for Harmonic Control in Electric Power Systems*. Accessed: Apr. 27, 2024. [Online]. Available: <https://ieeexplore.ieee.org/document/6826459>
- [30] M. Jiang, J. Tian, H. H. Goh, J. Yi, S. Li, D. Zhang, and T. Wu, "Experimental study on the influence of high frequency PWM harmonics on the losses of induction motor," *Energy Rep.*, vol. 8, pp. 332–342, Nov. 2022.
- [31] A. Tripathi and G. Narayanan, "Torque ripple minimization in neutral-point-clamped three-level inverter fed induction motor drives operated at low-switching-frequency," in *Proc. Int. Symp. Power Electron., Electr. Drives, Autom. Motion (SPEDAM)*, Capri, Italy, Jun. 2016, pp. 728–733.
- [32] J. Holtz, "Pulsewidth modulation for electronic power conversion," *Proc. IEEE*, vol. 82, no. 8, pp. 1194–1214, Aug. 1994.
- [33] J. Holtz, "Advanced PWM and predictive control—An overview," *IEEE Trans. Ind. Electron.*, vol. 63, no. 6, pp. 3837–3844, Jun. 2016.
- [34] D. G. Holmes and T. A. Lipo, *Pulse Width Modulation for Power Converters Principles and Practice*, 1st ed., Hoboken, NJ, USA: Wiley, 2003.
- [35] N. Hartgenbusch, R. W. De Doncker, and A. Thunen, "Optimized pulse patterns for salient synchronous machines," in *Proc. 23rd Int. Conf. Electr. Mach. Syst. (ICEMS)*, Hamamatsu, Japan, Nov. 2020, pp. 359–364.
- [36] N. Hartgenbusch, D. Pham, and R. W. De Doncker, "Synchronous optimal pulse width modulation for salient permanent magnet synchronous machines considering spatial harmonics," in *Proc. 25th Int. Conf. Electr. Mach. Syst. (ICEMS)*, Chiang Mai, Thailand, Nov. 2022, pp. 1–6.
- [37] Y.-C. Kwon, S. Kim, and S.-K. Sul, "Six-step operation of PMSM with instantaneous current control," *IEEE Trans. Ind. Appl.*, vol. 50, no. 4, pp. 2614–2625, Jul. 2014.

- [38] D.-C. Lee and G.-M. Lee, "A novel overmodulation technique for space-vector PWM inverters," *IEEE Trans. Power Electron.*, vol. 13, no. 6, pp. 1144–1151, Nov. 1998.
- [39] S.-H. Kim, *Electric Motor Control: DC, AC, and BLDC Motors*, 1st ed., Amsterdam, The Netherlands: Elsevier, 2017.
- [40] D. G. Holmes, "The significance of zero space vector placement for carrier-based PWM schemes," *IEEE Trans. Ind. Appl.*, vol. 32, no. 5, pp. 1122–1129, Oct. 1996.
- [41] A. M. Hava, R. J. Kerkman, and T. A. Lipo, "A high-performance generalized discontinuous PWM algorithm," *IEEE Trans. Ind. Appl.*, vol. 34, no. 5, pp. 1059–1071, Oct. 1998.
- [42] J. Holtz, W. Lotzkat, and A. M. Khambadkone, "On continuous control of PWM inverters in the overmodulation range including the six-step mode," *IEEE Trans. Power Electron.*, vol. 8, no. 4, pp. 546–553, Oct. 1993.
- [43] H.-I. Jeong and S.-H. Kim, "Improved overmodulation technique for enhancing torque capability of inverter-driven AC motors," *J. Power Electron.*, vol. 21, no. 4, pp. 683–692, Apr. 2021.
- [44] H. Lee, S. Hong, J. Choi, K. Nam, and J. Kim, "Sector-based analytic overmodulation method," *IEEE Trans. Ind. Electron.*, vol. 66, no. 10, pp. 7624–7632, Oct. 2019.
- [45] P. Mattavelli, F. Polo, F. Dal Lago, and S. Saggini, "Analysis of control-delay reduction for the improvement of UPS voltage-loop bandwidth," *IEEE Trans. Ind. Electron.*, vol. 55, no. 8, pp. 2903–2911, Aug. 2008.
- [46] V. Blasko, V. Kaura, and W. Niewiadomski, "Sampling of discontinuous voltage and current signals in electrical drives: A system approach," *IEEE Trans. Ind. Appl.*, vol. 34, no. 5, pp. 1123–1130, Oct. 1998.
- [47] R. P. Aguilera, P. Acuña, P. Lezana, G. Konstantinou, B. Wu, S. Bernet, and V. G. Agelidis, "Selective harmonic elimination model predictive control for multilevel power converters," *IEEE Trans. Power Electron.*, vol. 32, no. 3, pp. 2416–2426, Mar. 2017.
- [48] A. Poorfakhraei, M. Narimani, and A. Emadi, "A review of modulation and control techniques for multilevel inverters in traction applications," *IEEE Access*, vol. 9, pp. 24187–24204, 2021.
- [49] A. Ahmed, S. P. Biswas, M. S. Anower, M. R. Islam, S. Mondal, and S. M. Muyeen, "A hybrid PWM technique to improve the performance of voltage source inverters," *IEEE Access*, vol. 11, pp. 4717–4729, 2023.
- [50] R. Alavathan and A. Kavitha, "Digital implementation of DS-SFH hybrid spread-spectrum modulation technique in three-phase voltage-source converter," *Electr. Eng.*, vol. 104, no. 3, pp. 1413–1423, Jun. 2022.
- [51] J. Caldwell. (2013). *Analog Pulse Width Modulation*. [Online]. Available: https://www.ti.com/lit/ug/slau508/slau508.pdf?ts=1716166162388&ref_url=https%253A%252F%252Fwww.google.com%252F
- [52] M. C. Trigg, H. Dehbonei, and C. V. Nayar, "Digital sinusoidal PWM generation using a low-cost micro-controller based single-phase inverter," in *Proc. IEEE Conf. Emerg. Technol. Factory Autom.*, vol. 1, Catania, Italy, Mar. 2005, pp. 393–396.
- [53] S. Albatran, A. S. Allabadi, A. R. A. Khalailah, and Y. Fu, "Improving the performance of a two-level voltage source inverter in the overmodulation region using adaptive optimal third harmonic injection pulsewidth modulation schemes," *IEEE Trans. Power Electron.*, vol. 36, no. 1, pp. 1092–1103, Jan. 2021.
- [54] A. Tripathi and G. Narayanan, "Evaluation and minimization of low-order harmonic torque in low-switching-frequency inverter-fed induction motor drives," *IEEE Trans. Ind. Appl.*, vol. 52, no. 2, pp. 1477–1488, Mar. 2016.
- [55] A. M. Hava, R. J. Kerkman, and T. A. Lipo, "Carrier-based PWM-VSI overmodulation strategies: Analysis, comparison, and design," *IEEE Trans. Power Electron.*, vol. 13, no. 4, pp. 674–689, Jul. 1998.
- [56] K. Kumar, P. Angel, J. John, and Kumar, "Simulation and comparison of SPWM and SVPWM control for three phase inverter," *ARNP J. Eng. Appl. Sci.*, vol. 5, pp. 1–12, Jan. 2010.
- [57] T. Sutikno, A. Jidin, and M. F. Basar, "Simple realization of 5-Segment discontinuous SVPWM based on FPGA," *Int. J. Comput. Electr. Eng.*, vol. 10, pp. 148–157, Mar. 2010.
- [58] S. Dusmez, L. Qin, and B. Akin, "A new SVPWM technique for DC negative rail current sensing at low speeds," *IEEE Trans. Ind. Electron.*, vol. 62, no. 2, pp. 826–831, Feb. 2015.
- [59] Y. Huang, Y. Xu, W. Zhang, and J. Zou, "Hybrid RPWM technique based on modified SVPWM to reduce the PWM acoustic noise," *IEEE Trans. Power Electron.*, vol. 34, no. 6, pp. 5667–5674, Jun. 2019.
- [60] W.-S. Jeong, Y.-S. Lee, J.-H. Lee, C.-H. Lee, and C.-Y. Won, "Space vector modulation (SVM)-based common-mode current (CMC) reduction method of H8 inverter for permanent magnet synchronous motor (PMSM) drives," *Energies*, vol. 15, no. 1, p. 266, Dec. 2021.
- [61] K. Zhou and D. Wang, "Relationship between space-vector modulation and three-phase carrier-based PWM: A comprehensive analysis [three-phase inverters]," *IEEE Trans. Ind. Electron.*, vol. 49, no. 1, pp. 186–196, Feb. 2002.
- [62] S. Hiti, D. Tang, C. Stancu, and E. Ostrom, "Zero vector modulation method for voltage source inverter operating near zero output frequency," in *Proc. Conf. Rec. IEEE Ind. Appl. Conf., 39th IAS Annu. Meeting.*, vol. 1, Seattle, WA, USA, Apr. 2004, pp. 171–176.
- [63] A. Birda, J. Reuss, and C. M. Hackl, "Synchronous optimal pulsewidth modulation for synchronous machines with highly operating point dependent magnetic anisotropy," *IEEE Trans. Ind. Electron.*, vol. 68, no. 5, pp. 3760–3769, May 2021.
- [64] A. Tripathi and G. Narayanan, "Optimal pulse width modulation of voltage-source inverter fed motor drives with relaxation of quarter wave symmetry condition," in *Proc. IEEE Int. Conf. Electron., Comput. Commun. Technol. (CONECCT)*, Jan. 2014, pp. 1–6.
- [65] A. K. Vijayan, D. Xiao, B. Batkhisig, A. D. Callegaro, R. Baranwal, and A. Emadi, "Comparative study on pulse pattern optimization for high-speed permanent magnet synchronous motors," in *Proc. IEEE Transp. Electrific. Conf. Expo (ITEC)*, Jun. 2022, pp. 708–713.
- [66] A. Birth, T. Geyer, H. D. T. Mouton, and M. Dorfling, "Generalized three-level optimal pulse patterns with lower harmonic distortion," *IEEE Trans. Power Electron.*, vol. 35, no. 6, pp. 5741–5752, Jun. 2020.
- [67] H. S. Patel and R. G. Hofit, "Generalized techniques of harmonic elimination and voltage control in thyristor inverters: Part I—Harmonic elimination," *IEEE Trans. Ind. Appl.*, vol. 1A-9, no. 3, pp. 310–317, May 1973.
- [68] H. S. Patel and R. G. Hofit, "Generalized techniques of harmonic elimination and voltage control in thyristor inverters: Part II—Voltage control techniques," *IEEE Trans. Ind. Appl.*, vol. 1A-10, no. 5, pp. 666–673, Sep. 1974.
- [69] J. R. Wells, B. M. Nee, P. L. Chapman, and P. T. Krein, "Selective harmonic control: A general problem formulation and selected solutions," *IEEE Trans. Power Electron.*, vol. 20, no. 6, pp. 1337–1345, Nov. 2005.
- [70] L. G. Franquelo, J. Napoles, R. C. P. Guisado, J. I. Leon, and M. A. Aguirre, "A flexible selective harmonic mitigation technique to meet grid codes in three-level PWM converters," *IEEE Trans. Ind. Electron.*, vol. 54, no. 6, pp. 3022–3029, Dec. 2007.
- [71] M. Hepp, M. Saur, W. Wondrak, and M.-M. Bakran, "Enhanced analytical models based on switching angles to evaluate the effects of optimized pulse patterns on the overall electric drive train," *IEEE Trans. Energy Convers.*, early access, Oct. 9, 2024, doi: [10.1109/TEC.2024.3476509](https://doi.org/10.1109/TEC.2024.3476509).
- [72] A. K. Vijayan, S. Chakkalakkal, and A. Emadi, "Efficiency evaluation of 800V electric vehicle powertrain using two-level voltage source inverter with different modulation techniques," in *Proc. IEEE Transp. Electrific. Conf. Expo (ITEC)*, Jun. 2023, pp. 1–6.
- [73] T. Geyer, P. Karamanakos, and I. Koukoulas, "Optimized pulse patterns with bounded semiconductor losses," *IEEE Trans. Power Electron.*, vol. 39, no. 3, pp. 3233–3243, Mar. 2024.
- [74] A. K. Vijayan, B. Batkhisig, P. F. D. C. Gonçalves, G. Pietrini, R. Baranwal, B. Nahid-Mobarakeh, and A. Emadi, "Torque harmonic minimization optimal pulse pattern modulation technique for permanent-magnet synchronous motors," *IEEE Trans. Transport. Electrific.*, early access, Jan. 29, 2025, doi: [10.1109/TTE.2025.3536163](https://doi.org/10.1109/TTE.2025.3536163).
- [75] M. Hepp, M. Saur, and M.-M. Bakran, "Reducing the DC-link voltage ripple by optimized pulse patterns to increase the power density of traction inverters in electric vehicles," *IEEE Open J. Power Electron.*, vol. 5, pp. 1767–1781, 2024.
- [76] S. Pan, K. Yang, M. Wu, X. Li, J. Wang, Y. W. Li, and W. Yu, "Switching frequency minimized harmonic mitigation: A multiobjective optimized modulation strategy for High-power converters," *IEEE Trans. Power Electron.*, vol. 38, no. 9, pp. 11080–11090, Sep. 2023.
- [77] P. N. Enjeti, P. D. Ziogas, and J. F. Lindsay, "Programmed PWM techniques to eliminate harmonics: A critical evaluation," *IEEE Trans. Ind. Appl.*, vol. 26, no. 2, pp. 302–316, Apr. 1990.
- [78] D. Bendib, C. Larbes, A. Guellal, M. Khider, and F. Akel, "FPGA-based implementation of online selective harmonic elimination PWM for voltage source inverter," *Int. J. Electron.*, vol. 104, no. 10, pp. 1715–1731, Oct. 2017.

- [79] A. Marquez Alcaide, J. I. Leon, M. Laguna, F. Gonzalez-Rodriguez, R. Portillo, E. Zafra-Ratia, S. Vazquez, L. G. Franquelo, S. Bayhan, and H. Abu-Rub, "Real-time selective harmonic mitigation technique for power converters based on the exchange market algorithm," *Energies*, vol. 13, no. 7, p. 1659, Apr. 2020.
- [80] F. Filho, L. M. Tolbert, Y. Cao, and B. Ozipineci, "Real-time selective harmonic minimization for multilevel inverters connected to solar panels using artificial neural network angle generation," *IEEE Trans. Ind. Appl.*, vol. 47, no. 5, pp. 2117–2124, Sep. 2011.
- [81] J. Hao, G. Zhang, K. Yang, M. Wu, Y. Zheng, and W. Hu, "Online unified solution for selective harmonic elimination based on stochastic configuration network and Levenberg–Marquardt algorithm," *IEEE Trans. Ind. Electron.*, vol. 69, no. 10, pp. 10724–10734, Oct. 2022.
- [82] J. Lago and M. L. Heldwein, "Generalized synchronous optimal pulse width modulation for multilevel inverters," *IEEE Trans. Power Electron.*, vol. 32, no. 8, pp. 6297–6307, Aug. 2017.
- [83] A. Edpuganti and A. K. Rathore, "A survey of low switching frequency modulation techniques for medium-voltage multilevel converters," *IEEE Trans. Ind. Appl.*, vol. 51, no. 5, pp. 4212–4228, Sep. 2015.
- [84] A. K. Rathore, J. Holtz, and T. Boller, "Generalized optimal pulsewidth modulation of multilevel inverters for low-switching-frequency control of medium-voltage high-power industrial AC drives," *IEEE Trans. Ind. Electron.*, vol. 60, no. 10, pp. 4215–4224, Oct. 2013.
- [85] S. Dai, J. Wang, Z. Sun, and E. Chong, "Mode transition of synchronous optimal modulation for high-speed PMSM drives," *IEEE Trans. Ind. Appl.*, vol. 58, no. 2, pp. 2001–2012, Mar. 2022.
- [86] M. Steczek, P. Chudzik, and A. Szlag, "Combination of SHE- and SHM-PWM techniques for VSI DC-link current harmonics control in railway applications," *IEEE Trans. Ind. Electron.*, vol. 64, no. 10, pp. 7666–7678, Oct. 2017.
- [87] M. P. Kazmierkowski and L. Malesani, "Current control techniques for three-phase voltage-source PWM converters: A survey," *IEEE Trans. Ind. Electron.*, vol. 45, no. 5, pp. 691–703, Oct. 1998.
- [88] Z. Yu, A. Mohammed, and I. Panahi, "A review of three PWM techniques," in *Proc. Amer. Control Conf.*, vol. 1, 1997, pp. 257–261.
- [89] J. Rodríguez, J. Pontt, C. Silva, P. Cortés, U. Amman, and S. Rees, "Predictive current control of a voltage source inverter," *IEEE Trans. Ind. Electron.*, vol. 54, no. 1, pp. 495–503, Feb. 2007.
- [90] B. Batkhisig, P. F. da Costa Gonçalves, G. Pietrini, B. Nahid-Mobarakeh, R. Baranwal, and A. Emadi, "Enhanced hybrid PWM for the closed-loop control of permanent magnet synchronous motor drives," *IEEE Trans. Transport. Electric.*, vol. 11, no. 1, pp. 3785–3795, Feb. 2025.
- [91] J. Plotkin, U. Schaefer, and R. Hanitsch, "Torque ripple in PWM-VSI-fed drives due to parasitic effects in the inverter control," in *Proc. 35th Annu. Conf. IEEE Ind. Electron.*, Porto, Portugal, Nov. 2009, pp. 1368–1372.
- [92] F. Xie, W. Wu, W. Hong, and C. Qiu, "Torque ripple suppression strategy of asynchronous motor for electric vehicle based on random pulse position space vector pulse width modulation with uniform probability density," *IET Electr. Power Appl.*, vol. 15, no. 8, pp. 1068–1080, Aug. 2021.
- [93] P. Stumpf, R. K. Járđán, and I. Nagy, "Comparison of naturally sampled PWM techniques in ultrahigh speed drives," in *Proc. IEEE Int. Symp. Ind. Electron.*, Hangzhou, China, May 2012, pp. 246–251.
- [94] *Silicon Carbide (SiC) Power Modules | Wolfspeed*. Accessed: Mar. 3, 2025. [Online]. Available: <https://www.wolfspeed.com/products/power/sic-power-modules/>
- [95] H.-P. To, M. F. Rahman, and C. Grantham, "Time delay compensation for a DSP-based current-source converter using observer-predictor controller," in *Proc. 7th Int. Conf. Power Electron. Drive Syst.*, Bangkok, Thailand, Nov. 2007, pp. 1091–1096.
- [96] C. Xue, L. Ding, Z. Quan, and Y. Li, "Multirate modeling and predictive control for WBG-device-based high-switching-frequency power converters," *IEEE Trans. Ind. Electron.*, vol. 71, no. 1, pp. 93–103, Jan. 2024.
- [97] F. Nejabatkhah, Y. W. Li, and H. Tian, "Power quality control of smart hybrid AC/DC microgrids: An overview," *IEEE Access*, vol. 7, pp. 52295–52318, 2019.
- [98] L. Saribulut and M. Tümay, "Robust space vector modulation technique for unbalance voltage disturbances," *Electr. Power Syst. Res.*, vol. 80, no. 11, pp. 1364–1374, Nov. 2010.
- [99] H. Hu, H. Wang, K. Liu, J. Wei, and X. Shen, "A simplified space vector pulse width modulation algorithm of a high-speed permanent magnet synchronous machine drive for a flywheel energy storage system," *Energies*, vol. 15, no. 11, p. 4065, Jun. 2022.
- [100] R. P. Aguilera, P. Lezana, G. Konstantinou, P. Acuna, B. Wu, S. Bernet, and V. G. Agelidis, "Closed-loop SHE-PWM technique for power converters through model predictive control," in *Proc. 41st Annu. Conf. IEEE Ind. Electron. Soc.*, Nov. 2015, pp. 5261–5266.
- [101] D. Xiao, B. Batkhisig, A. K. Vijayan, A. D. Callegaro, R. Baranwal, and A. Emadi, "Model-free predictive pulse pattern control for permanent magnet synchronous motor drives," in *Proc. IEEE Energy Convers. Congr. Expo. (ECCE)*, Oct. 2022, pp. 1–5.
- [102] L. Rosado, J. Samanes, E. Gubia, and J. Lopez, "Selective harmonic mitigation: Limitations of classical control strategies and benefits of model predictive control," *IEEE Trans. Ind. Appl.*, vol. 59, no. 5, pp. 6082–6094, Sep. 2023.
- [103] B. Batkhisig, P. F. Da Costa Gonçalves, B. Nahid-Mobarakeh, and A. Emadi, "Look-up table size reduction strategy for synchronous optimal pulse width modulation," in *Proc. IEEE Energy Convers. Congr. Expo. (ECCE)*, Oct. 2023, pp. 4851–4855.
- [104] A. K. Rathore, J. Holtz, and T. Boller, "Synchronous optimal pulsewidth modulation for low-switching-frequency control of medium-voltage multilevel inverters," *IEEE Trans. Ind. Electron.*, vol. 57, no. 7, pp. 2374–2381, Jul. 2010.
- [105] H. Su, G. Jie, L. Zhou, J. Han, Q. Meng, W. Li, and C. Liu, "Stator flux trajectory control with optimized pulse patterns based on voltage command feed-forward," in *Proc. IEEE 3rd Int. Electr. Energy Conf. (CIEEC)*, Beijing, China, Sep. 2019, pp. 662–667.
- [106] M. A. W. Begh, P. Karamanakos, and T. Geyer, "Gradient-based predictive pulse pattern control of medium-voltage drives—Part I: Control, concept, and analysis," *IEEE Trans. Power Electron.*, vol. 37, no. 12, pp. 14222–14236, Dec. 2022.
- [107] J. Holtz and N. Oikonomou, "Fast dynamic control of medium voltage drives operating at very low switching frequency—An overview," *IEEE Trans. Ind. Electron.*, vol. 55, no. 3, pp. 1005–1013, Mar. 2008.
- [108] T. Geyer, N. Oikonomou, G. Papafotiou, and F. D. Kieferndorf, "Model predictive pulse pattern control," *IEEE Trans. Ind. Appl.*, vol. 48, no. 2, pp. 663–676, Mar. 2012.
- [109] K. W. Schachter and B. A. Fortman. (2020). *Flexible PWMs Enable Multi-Axis Drives, Multi-Level Inverters*. Texas Instrum. [Online]. Available: https://www.ti.com/lit/an/sprt723b/sprt723b.pdf?ts=1714515031300&ref_url=https%253A%252F%252Fwww.google.com%252F
- [110] R. Xie, Y. Wu, B. Lin, O. Xu, Y. He, and L. Shen, "A regular sampling method based on the immediate mode for improving the stability of inverters," *Energy Rep.*, vol. 9, pp. 305–315, Sep. 2023.
- [111] C. Chen, J. Xiong, Z. Wan, J. Lei, and K. Zhang, "A time delay compensation method based on area equivalence for active damping of an LCL-Type converter," *IEEE Trans. Power Electron.*, vol. 32, no. 1, pp. 762–772, Jan. 2017.
- [112] F. Briz, D. Díaz-Reigosa, M. W. Degner, P. García, and J. M. Guerrero, "Current sampling and measurement in PWM operated AC drives and power converters," in *Proc. Int. Power Electron. Conf.*, Jun. 2010, pp. 2753–2760.
- [113] H. Tian, Y. W. Li, and Q. Zhao, "Multirate harmonic compensation control for low switching frequency converters: Scheme, modeling, and analysis," *IEEE Trans. Power Electron.*, vol. 35, no. 4, pp. 4143–4156, Apr. 2020.
- [114] M.-F. Tsai, C.-S. Tseng, and P.-J. Cheng, "Implementation of an FPGA-based current control and SVPWM ASIC with asymmetric five-segment switching scheme for AC motor drives," *Energies*, vol. 14, no. 5, p. 1462, Mar. 2021.
- [115] A. M. Hava and N. O. Çetin, "A generalized scalar PWM approach with easy implementation features for three-phase, three-wire voltage-source inverters," *IEEE Trans. Power Electron.*, vol. 26, no. 5, pp. 1385–1395, May 2011.
- [116] R. Baranwal, K. Basu, and N. Mohan, "Carrier-based implementation of SVPWM for dual two-level VSI and dual matrix converter with zero common-mode voltage," *IEEE Trans. Power Electron.*, vol. 30, no. 3, pp. 1471–1487, Mar. 2015.
- [117] C. Wang, Q. Zhang, W. Yu, and K. Yang, "A comprehensive review of solving selective harmonic elimination problem with algebraic algorithms," *IEEE Trans. Power Electron.*, vol. 39, no. 1, pp. 850–868, Jan. 2024.

- [118] G. Silva, B. Batkhisig, D. Wang, G. Pietrini, P. Suntharalingam, and A. Emadi, "Application of optimized pulse pattern modulation to 1 MVA three-level aerospace inverters," in *Proc. IEEE Energy Convers. Congr. Expo. (ECCE)*, Oct. 2024, pp. 2513–2516. [Online]. Available: <https://ieeexplore.ieee.org/document/10861126/?arnumber=10861126>
- [119] C. Zou, "Optimized pulse pattern control strategy investigation on signal level hardware in the loop," M.S. thesis, Dept. Elect. Eng., Chalmers Univ. Technol., Gothenburg, Sweden, 2023.
- [120] B. Batkhisig, D. Xiao, A. K. Vijayan, A. D. Callegaro, R. Baranwal, and A. Emadi, "Hysteresis synchronous optimal PWM with continuous switching angles for PMSMs," in *Proc. 48th Annu. Conf. IEEE Ind. Electron. Soc.*, Oct. 2022, pp. 1–6.
- [121] N. Hartgenbusch, I. Ralev, R. W. De Doncker, and T. Kojima, "Stator flux trajectory control combined with optimized pulse patterns for interior permanent magnet machines," in *Proc. 22nd Int. Conf. Electr. Mach. Syst. (ICEMS)*, Aug. 2019, pp. 1–6.
- [122] F. Mink, K. Peter, H. Kasten, and S. Beineke, "Feedback control of high-speed PMSM with synchronous optimal PWM," in *Proc. 18th Eur. Conf. Power Electron. Appl. (EPE ECCE Europe)*, Sep. 2016, pp. 1–10.
- [123] L. Diao, J. Tang, P. C. Loh, S. Yin, L. Wang, and Z. Liu, "An efficient DSP-FPGA-based implementation of hybrid PWM for electric rail traction induction motor control," *IEEE Trans. Power Electron.*, vol. 33, no. 4, pp. 3276–3288, Apr. 2018.
- [124] J. Cheng, T. Xu, D. Chen, and G. Chen, "Dynamic and steady state response analysis of selective harmonic elimination in high power inverters," *IEEE Access*, vol. 9, pp. 75588–75598, 2021.
- [125] J. Holtz and N. Oikonomou, "Estimation of the fundamental current in low-switching-frequency high dynamic medium-voltage drives," *IEEE Trans. Ind. Appl.*, vol. 44, no. 5, pp. 1597–1605, Sep. 2008.
- [126] T. Dorfling, H. D. T. Mouton, and T. Geyer, "Generalized model predictive pulse pattern control based on small-signal modeling—Part 1: Algorithm," *IEEE Trans. Power Electron.*, vol. 37, no. 9, pp. 10476–10487, Sep. 2022.
- [127] A. Birda, J. Reuss, and C. M. Hackl, "Simple fundamental current estimation and smooth transition between synchronous optimal PWM and asynchronous SVM," *IEEE Trans. Ind. Electron.*, vol. 67, no. 8, pp. 6354–6364, Aug. 2020.
- [128] N. Oikonomou and J. Holtz, "Closed-loop control of medium-voltage drives operated with synchronous optimal pulsewidth modulation," *IEEE Trans. Ind. Appl.*, vol. 44, no. 1, pp. 115–123, Jan. 2008.
- [129] B. Bilgin, P. Magne, P. Malysz, Y. Yang, V. Pantelic, M. Preindl, A. Korobkine, W. Jiang, M. Lawford, and A. Emadi, "Making the case for electrified transportation," *IEEE Trans. Transport. Electric.*, vol. 1, no. 1, pp. 4–17, Jun. 2015.
- [130] J. Chen, R. Ni, T. Li, R. Qiu, and Z. Liu, "The harmonic characteristic of the advanced synchronous SVPWM overmodulation strategy," *IEEE Access*, vol. 7, pp. 148934–148949, 2019.
- [131] K. He, J. Li, L. Xiao, Y. Lu, L. Wu, and H. Chen, "Synchronous optimal PWM with continuous switching-to-fundamental frequency ratio," *IEEE J. Emerg. Sel. Topics Power Electron.*, vol. 11, no. 2, pp. 1466–1476, Apr. 2023.
- [132] H. Yang, Y. Zhang, G. Yuan, P. D. Walker, and N. Zhang, "Hybrid synchronized PWM schemes for closed-loop current control of high-power motor drives," *IEEE Trans. Ind. Electron.*, vol. 64, no. 9, pp. 6920–6929, Sep. 2017.
- [133] *Global EV Outlook 2019—Analysis*. Accessed: Apr. 29, 2024. [Online]. Available: <https://www.iea.org/reports/global-ev-outlook-2019>
- [134] N. Keshmiri, D. Wang, B. Agrawal, R. Hou, and A. Emadi, "Current status and future trends of GaN HEMTs in electrified transportation," *IEEE Access*, vol. 8, pp. 70553–70571, 2020.
- [135] I. V. Alexandrov and I. A. Bahovtsev, "Combined PWM algorithm for voltage source inverter with microprocessor control system," in *Proc. 20th Int. Conf. Young Specialists Micro/Nanotechnologies Electron Devices (EDM)*, Jun. 2019, pp. 580–585.
- [136] W. Kekang, T. Q. Zheng, R. Wang, and W. Chenchen, "Study on a hybrid PWM method under low switching frequency," in *Proc. Int. Conf. Electr. Mach. Syst.*, Beijing, China, Aug. 2011, pp. 1–4.
- [137] M. Hepp, K. Kaiser, M. Saur, and M.-M. Bakran, "Detailed analysis of optimized pulse patterns interacting with salient PMSMs applying different symmetry conditions," *IEEE Open J. Power Electron.*, vol. 5, pp. 1280–1296, 2024.
- [138] I. Husain, B. Ozpineci, M. S. Islam, E. Gurbinar, G.-J. Su, W. Yu, S. Chowdhury, L. Xue, D. Rahman, and R. Sahu, "Electric drive technology trends, challenges, and opportunities for future electric vehicles," *Proc. IEEE*, vol. 109, no. 6, pp. 1039–1059, Jun. 2021.
- [139] X. Yuan, I. Laird, and S. Walder, "Opportunities, challenges, and potential solutions in the application of fast-switching SiC power devices and converters," *IEEE Trans. Power Electron.*, vol. 36, no. 4, pp. 3925–3945, Apr. 2021.
- [140] J. Hobraiche, J. P. Vilain, and C. Plasse, "Offline optimized pulse pattern with a view to reducing DC-link capacitor application to a starter generator," in *Proc. IEEE 35th Annu. Power Electron. Specialists Conf.*, Jul. 2004, pp. 3336–3341.
- [141] A. M. Cross, P. D. Evans, and A. J. Forsyth, "DC link current in PWM inverters with unbalanced and non-linear loads," *IEE Proc. Electr. Power Appl.*, vol. 146, no. 6, p. 620, 1999.
- [142] S. Li, L. Yang, and T. Wang, "Analysis of the DC-link voltage ripple for the three-phase voltage source converter under nonlinear output current," *Energies*, vol. 15, no. 8, p. 2892, Apr. 2022.
- [143] A. Birda, C. Grabher, C. M. Hackl, and J. Reuss, "DC-link capacitor and inverter current ripples in anisotropic synchronous motor drives produced by synchronous optimal PWM," *IEEE Trans. Ind. Electron.*, vol. 69, no. 5, pp. 4484–4494, May 2022.
- [144] D. Han, S. Li, Y. Wu, W. Choi, and B. Sarlioglu, "Comparative analysis on conducted CM EMI emission of motor drives: WBG versus Si devices," *IEEE Trans. Ind. Electron.*, vol. 64, no. 10, pp. 8353–8363, Oct. 2017.
- [145] C.-C. Hou, C.-C. Shih, P.-T. Cheng, and A. M. Hava, "Common-mode voltage reduction pulsewidth modulation techniques for three-phase grid-connected converters," *IEEE Trans. Power Electron.*, vol. 28, no. 4, pp. 1971–1979, Apr. 2013.
- [146] J.-H. Im, J.-K. Kang, Y.-K. Lee, and J. Hur, "Shaft voltage elimination method to reduce bearing faults in dual three-phase motor," *IEEE Access*, vol. 10, pp. 81042–81053, 2022.
- [147] C. Buccella, C. Cecati, and H. Latafat, "Digital control of power converters—A survey," *IEEE Trans. Ind. Informat.*, vol. 8, no. 3, pp. 437–447, Aug. 2012.
- [148] Z. Cao, J. Mao, X. Dong, R. Madonski, C. Zhang, and J. Yang, "Composite generalized dynamic predictive control with self-tuning horizon for wide-range speed regulation of PMSM drives," *IEEE Trans. Energy Convers.*, vol. 39, no. 1, pp. 659–674, Mar. 2024.
- [149] J. Kim, S.-W. Ryu, M. S. Rifaq, H. H. Choi, and J.-W. Jung, "Improved torque ripple minimization technique with enhanced efficiency for surface-mounted PMSM drives," *IEEE Access*, vol. 8, pp. 115017–115027, 2020.
- [150] P. P. Patel and M. A. Mulla, "A single carrier-based pulsewidth modulation technique for three-to-three phase indirect matrix converter," *IEEE Trans. Power Electron.*, vol. 35, no. 11, pp. 11589–11601, Nov. 2020.
- [151] K. Shenai, "Future prospects of widebandgap (WBG) semiconductor power switching devices," *IEEE Trans. Electron Devices*, vol. 62, no. 2, pp. 248–257, Feb. 2015.
- [152] A. K. Morya, M. C. Gardner, B. Anvari, L. Liu, A. G. Yepes, J. Doval-Gandoy, and H. A. Toliyat, "Wide bandgap devices in AC electric drives: Opportunities and challenges," *IEEE Trans. Transport. Electric.*, vol. 5, no. 1, pp. 3–20, Mar. 2019.
- [153] H. Yuruk, O. Keysan, and B. Ulutas, "Comparison of the effects of nonlinearities for Si MOSFET and GaN E-HEMT based VSIs," *IEEE Trans. Ind. Electron.*, vol. 68, no. 7, pp. 5606–5615, Jul. 2021.
- [154] B. Zhang and S. Wang, "A survey of EMI research in power electronics systems with wide-bandgap semiconductor devices," *IEEE J. Emerg. Sel. Topics Power Electron.*, vol. 8, no. 1, pp. 626–643, Mar. 2020.
- [155] X. Li, F. Xiao, Y. Luo, R. Wang, and Z. Shi, "An improved equivalent circuit model of SiC MOSFET and its switching behavior predicting method," *IEEE Trans. Ind. Electron.*, vol. 69, no. 9, pp. 9462–9471, Sep. 2022.
- [156] T. Liu, T. T. Y. Wong, and Z. J. Shen, "A survey on switching oscillations in power converters," *IEEE J. Emerg. Sel. Topics Power Electron.*, vol. 8, no. 1, pp. 893–908, Mar. 2020.
- [157] B. Narayanasamy, A. S. Sathyanarayanan, F. Luo, and C. Chen, "Reflected wave phenomenon in SiC motor drives: Consequences, boundaries, and mitigation," *IEEE Trans. Power Electron.*, vol. 35, no. 10, pp. 10629–10642, Oct. 2020.

- [158] J. Rodriguez et al., "Latest advances of model predictive control in electrical drives—Part I: Basic concepts and advanced strategies," *IEEE Trans. Power Electron.*, vol. 37, no. 4, pp. 3927–3942, Apr. 2022.
- [159] P. F. C. Gonçalves, S. M. A. Cruz, and A. M. S. Mendes, "Disturbance observer based predictive current control of six-phase permanent magnet synchronous machines for the mitigation of steady-state errors and current harmonics," *IEEE Trans. Ind. Electron.*, vol. 69, no. 1, pp. 130–140, Jan. 2022.
- [160] P. F. C. Gonçalves, S. M. A. Cruz, and A. M. S. Mendes, "Multistage predictive current control based on virtual vectors for the reduction of current harmonics in six-phase PMSMs," *IEEE Trans. Energy Convers.*, vol. 36, no. 2, pp. 1368–1377, Jun. 2021.
- [161] P. Karamanakos and T. Geyer, "Guidelines for the design of finite control set model predictive controllers," *IEEE Trans. Power Electron.*, vol. 35, no. 7, pp. 7434–7450, Jul. 2020.
- [162] P. Karamanakos, E. Liegmann, T. Geyer, and R. Kennel, "Model predictive control of power electronic systems: Methods, results, and challenges," *IEEE Open J. Ind. Appl.*, vol. 1, pp. 95–114, 2020.
- [163] E. Zafra, S. Vazquez, T. Geyer, R. P. Aguilera, and L. G. Franquelo, "Long prediction horizon FCS-MPC for power converters and drives," *IEEE Open J. Ind. Electron. Soc.*, vol. 4, pp. 159–175, 2023.
- [164] T. Dorfling, H. du Toit Mouton, T. Geyer, and P. Karamanakos, "Long-horizon finite-control-set model predictive control with nonrecursive sphere decoding on an FPGA," *IEEE Trans. Power Electron.*, vol. 35, no. 7, pp. 7520–7531, Jul. 2020.
- [165] M. Vasiladiotis, A. Christe, and T. Geyer, "Model predictive pulse pattern control for modular multilevel converters," *IEEE Trans. Ind. Electron.*, vol. 66, no. 3, pp. 2423–2431, Mar. 2019.
- [166] *ABB Introduces ACS6080 Drive for High Performance Motor Control*. Accessed: Apr. 19, 2024. [Online]. Available: <https://new.abb.com/new/detail/16575/abb-introduces-acs6080-drive-for-high-performance-motor-control>
- [167] V. Spudic and T. Geyer, "Model predictive control based on optimized pulse patterns for modular multilevel converter STATCOM," *IEEE Trans. Ind. Appl.*, vol. 55, no. 6, pp. 6137–6149, Nov. 2019.
- [168] S. Richter, T. Geyer, and M. Morari, "Resource-efficient gradient methods for model predictive pulse pattern control on an FPGA," *IEEE Trans. Control Syst. Technol.*, vol. 25, no. 3, pp. 828–841, May 2017.
- [169] M. Zhang, M. Yuan, and J. Jiang, "A comprehensive review of the multiphase motor drive topologies for high-power electric vehicle: Current status, research challenges, and future trends," *IEEE Trans. Transport. Electrification*, vol. 11, no. 1, pp. 3631–3654, Feb. 2025.
- [170] E. Sayed, M. Abdalmagid, G. Pietrini, N.-M. Sa'adeh, A. D. Callegaro, C. Goldstein, and A. Emadi, "Review of electric machines in more-hybrid-turbo-electric aircraft," *IEEE Trans. Transport. Electrification*, vol. 7, no. 4, pp. 2976–3005, Dec. 2021.
- [171] P. F. C. Gonçalves, S. M. A. Cruz, and A. M. S. Mendes, "Fault-tolerant predictive current control of six-phase PMSMs with minimal reconfiguration requirements," *IEEE J. Emerg. Sel. Topics Power Electron.*, vol. 11, no. 2, pp. 2084–2093, Apr. 2023.
- [172] P. F. C. Gonçalves, S. M. A. Cruz, and A. M. S. Mendes, "Fault-tolerant predictive current control of six-phase PMSMs with a single isolated neutral configuration," *Machines*, vol. 10, no. 12, Dec. 2022, Art. no. 1152.
- [173] M. J. Duran, E. Levi, and F. Barrero, "Multiphase electric drives: Introduction," in *Wiley Encyclopedia of Electrical and Electronics Engineering*. Hoboken, NJ, USA: Wiley, 2017, pp. 1–26.
- [174] E. Levi, "Multiphase electric machines for variable-speed applications," *IEEE Trans. Ind. Electron.*, vol. 55, no. 5, pp. 1893–1909, May 2008.
- [175] E. Levi, "Advances in converter control and innovative exploitation of additional degrees of freedom for multiphase machines," *IEEE Trans. Ind. Electron.*, vol. 63, no. 1, pp. 433–448, Jan. 2016.
- [176] W. Taha, P. Azer, A. D. Callegaro, and A. Emadi, "Multiphase traction inverters: State-of-the-art review and future trends," *IEEE Access*, vol. 10, pp. 4580–4599, 2022.
- [177] S. Paul and K. Basu, "Linear PWM techniques of asymmetrical six-phase machine with optimal current ripple performance," *IEEE Trans. Ind. Electron.*, vol. 70, no. 2, pp. 1298–1309, Feb. 2023.
- [178] L. Vancini, M. Mengoni, G. Rizzoli, G. Sala, L. Zarri, and A. Tani, "Carrier-based PWM overmodulation strategies for five-phase inverters," *IEEE Trans. Power Electron.*, vol. 36, no. 6, pp. 6988–6999, Jun. 2021.
- [179] M. Medina-Sánchez, A. G. Yepes, Ó. López, and J. Doval-Gandoy, "Comprehensive comparative assessment of multiphase overmodulation techniques and three-phase discontinuous PWM methods applied to symmetrical six-phase induction motor drives under overmodulation," *IEEE J. Emerg. Sel. Topics Power Electron.*, vol. 13, no. 1, pp. 702–720, Feb. 2025.
- [180] H. M. Eldeeb, A. S. Abdel-Khalik, and C. M. Hackl, "Postfault full torque–speed exploitation of dual three-phase IPMSM drives," *IEEE Trans. Ind. Electron.*, vol. 66, no. 9, pp. 6746–6756, Sep. 2019.
- [181] Y. Wang, X. Wen, and F. Zhao, "Vector control of six-phase PMSMs with selective harmonic elimination PWM," in *Proc. IEEE Conf. Expo Transp. Electrification Asia-Pacific (ITEC Asia-Pacific)*, Aug. 2014, pp. 1–6.
- [182] G. Liang, S. Huang, W. Liao, Z. Zhang, Y. Liu, C. Feng, X. Wu, and S. Huang, "An optimized modulation of torque and current harmonics suppression for dual three-phase PMSM," *IEEE Trans. Transport. Electrification*, vol. 10, no. 2, pp. 3443–3454, Jun. 2024.
- [183] G. Liang, W. Liao, Z. Zhang, D. Ni, S. Huang, M. Li, Y. Wen, and J. Gao, "An optimized pulsewidth modulation for dual three-phase PMSM under low carrier ratio," *IEEE Trans. Power Electron.*, vol. 37, no. 3, pp. 3062–3072, Mar. 2022.
- [184] M. Gu, Z. Wang, P. Liu, and J. He, "Comparative study of advanced modulation and control schemes for dual three-phase PMSM drives with low switching frequencies," *IEEE Trans. Transport. Electrification*, vol. 10, no. 1, pp. 962–975, Mar. 2024.



BATTUR BATKHISHIG (Member, IEEE) received the M.Eng. degree in electrical, electronics and information engineering from Nagaoka University of Technology, Nagaoka, Niigata, Japan, in 2018, and the Ph.D. degree in electrical and computer engineering from McMaster University, Hamilton, ON, Canada, in 2024. From 2013 to 2016 and from 2018 to 2020, he was an Electrical Engineer and later as an Electrical Engineering Supervisor with Uduu Engineering LLC, Ulaanbaatar, Mongolia. He is currently a Postdoctoral Fellow with the McMaster Automotive Resource Centre, McMaster University. His research interests include motor drives, PWM techniques, permanent magnet synchronous motor control, and electrified transportation.



PEDRO F. DA COSTA GONÇALVES (Member, IEEE) was born in Coimbra, Portugal. He received the M.Sc. and Ph.D. degrees in electrical and computer engineering from the University of Coimbra, Portugal, in 2013 and 2022, respectively. From 2014 to 2015, he was a Research Assistant with ENDIPREV S.A., with a focus on condition monitoring of DFIGs in wind generators. From June 2022 to June 2024, he was a Postdoctoral Research Fellow with the McMaster Automotive Resource Centre (MARC), Hamilton, ON, Canada, where he specialized in electric motor control for aerospace and automotive applications. Since July 2024, he has been an Assistant Lead Converter Control Engineer with the Research and Development Department, Vestas Wind Systems A/S, with a focus on the control of the grid-side converter of wind turbines. His main research interests include digital control, model predictive control, fault diagnosis, and fault-tolerant control applied to power converters and both three-phase and multiphase electric drives. In 2023, he was awarded the Best Ph.D. Thesis Award by IEEE Portugal for his thesis entitled "Fault-Tolerant Predictive Control of PMSGs in Offshore Wind Turbines."



GIORGIO PIETRINI (Member, IEEE) received the B.Sc., M.Sc., and Ph.D. degrees in information technology from the Department of Information Engineering, University of Parma, Parma, Italy, in 2009, 2014, and March 2019, respectively.

In May 2019, he joined the McMaster Automotive Resource Centre (MARC), McMaster University, Hamilton, ON, Canada, as a Postdoctoral Fellow. His main research interests include electrical machine design and modeling with special regard to permanent magnet synchronous motors for high-performance automotive traction and aerospace applications.



BABAK NAHID-MOBARAKEH (Fellow, IEEE) received the Ph.D. degree (Hons.) in electrical engineering from the Institut National Polytechnique de Lorraine, Nancy, France, in 2001, and the H.D.R. (Habilitation) degree (Hons.) in electrical engineering from the University of Lorraine, Nancy, in 2012. From 2001 to 2006, he was with the Centre de Robotique, Electrotechnique et Automatique, University of Picardie, Amiens, France. In September 2006, he joined the Ecole

Nationale Supérieure d'Electricité et de Mécanique, University of Lorraine, where he was a Professor, until December 2019. Since January 2020, he has been a Professor with McMaster University, Hamilton, ON, Canada. He has authored or co-authored more than 300 international peer-reviewed journal articles and conference papers as well as several book chapters. He holds 28 published patents. His main research interests include nonlinear and robust control design for power converters and motor drives, fault detection and fault-tolerant control of electric systems, and design, control, and stabilization of microgrids. He is a member of the Power Electronics and Motion Control (PEMC) Council. He was a recipient of several IEEE awards. He has chaired several conferences in the area of the control and electrification of transportation systems. From 2012 to 2019, he was an Executive Officer and then the Chair of the Industrial Automation and Control Committee (IACC) of the IEEE Industry Applications Society (IAS). He was also the IACC Committee Administrator and the Technical Committee Paper Review Chair of the IEEE IAS. He is the Chair of the IEEE Power Electronics Society Technical Committee on Electrified Transportation Systems (PELS TC4).



ALI EMADI (Fellow, IEEE) received the B.S. and M.S. degrees (Hons.) in electrical engineering from the Sharif University of Technology, Tehran, Iran, in 1995 and 1997, respectively, and the Ph.D. degree in electrical engineering from Texas A&M University, College Station, TX, USA, in 2000. He is currently Canada Excellence Research Chair Laureate with McMaster University, Hamilton, ON, Canada. He is also the holder of Canada Research Chair in Transportation Electrification

and Smart Mobility. Before joining McMaster University, he was the Harris Perlstein Endowed Chair Professor of Engineering and the Director of the Electric Power and Power Electronics Center and Grainger Laboratories, Illinois Institute of Technology, Chicago, IL, USA, where he established research and teaching facilities as well as courses in power electronics, motor drives, and vehicular power systems. He was the Founder, the Chair of the Board of Directors, and the President of Hybrid Electric Vehicle Technologies, Inc. (HEVT)—a university spin-off company of Illinois Tech. He is also the Founder, the President, and the Chief Executive Officer of Enedym Inc., and the Founder and the Chair of the Board of Directors of Menlolab Inc.—two McMaster University spin-off companies. He is the principal author/co-author of over 750 journal articles and conference papers as well as several books, including *Vehicular Electric Power Systems* (2003), *Energy Efficient Electric Motors* (2004), *Uninterruptible Power Supplies and Active Filters* (2004), *Modern Electric, Hybrid Electric, and Fuel Cell Vehicles* (2nd edition, 2009), and *Integrated Power Electronic Converters and Digital Control* (2009). He was the Inaugural General Chair of the 2012 IEEE Transportation Electrification Conference and Expo (ITEC) and has chaired several IEEE and SAE conferences in the areas of vehicle power and propulsion. He is also an Editor of the *Handbook of Automotive Power Electronics and Motor Drives* (2005) and *Advanced Electric Drive Vehicles* (2014). He is the Co-Editor of the *Switched Reluctance Motor Drives* (2018). He was the Founding Editor-in-Chief of IEEE TRANSACTIONS ON TRANSPORTATION ELECTRIFICATION, from 2014 to 2020.

...